



ICEBE
IMAGINEERING
NATURE



BEST
Bioenergy and
Sustainable Technologies

DIPLOMARBEIT

Gas cleaning from sulfur- and nitrogen compounds of product gases from dual fluidized bed steam gasification via adsorption

ausgeführt zum Zwecke der Erlangung des akademischen Grades eines
Diplomingenieurs unter der Leitung von

Univ.Prof. Dipl.-Ing. Dr.techn. Hermann Hofbauer

am

Institut für Verfahrenstechnik, Umwelttechnik und Technische Biowissenschaften

betreut von

Dipl.-Ing. Florian Benedikt

Dipl.-Ing. Alexander Bartik

Dipl.-Ing. Jürgen Loipersböck

eingereicht an der Technischen Universität Wien

Fakultät für Maschinenwesen und Betriebswissenschaften

von

Martín Leciñena

Matrikelnummer 11929173

Sonnenallee 30

1220 Wien

Wien, am 20.07.2020

Vorwort

Firstly, and most of all, I would like to thank Dipl.-Ing. Florian Benedikt, Dipl.-Ing. Alexander Bartik and Dipl.-Ing. Jürgen Loipersböck for their assistance, guidance and patience during the process of writing my project.

Additionally, I would like to thank the people at the gasification and gas-cleaning group for making my stay more enjoyable.

I would also like to extend my gratitude to my family and friends for their moral and material assistance. Special mention goes to Alejandra Franco, whose affection and knowledge provided unfailing encouragement and support.

Abstract

Climate change is one of the biggest issues that we must face as a society. The emission of greenhouse gases (GHG) such as CO₂ has led to the development of renewable energy technologies that avoid the emission of contaminant gases. The target of the European Commission is to reduce greenhouse gas emissions by at least 40% by 2030 compared with 1990 levels. Nevertheless, the last results from 2018 showed that the GHG emissions across the European Union had fallen by 23 % compared with 1990 levels. For this reason, further development of renewable energy technologies is mandatory to replace fossil fuels.

To decrease CO₂ emissions, the use of biomass gasification has been proposed. Nevertheless, it is still an expensive technology compared to the use of fossil fuels. Further research on proper measurement systems is needed in order to increase the competitiveness of this alternative. For this reason, the aim of the present project is to conduct a bibliographical research about nitrogen and sulfur measurement technologies in order to select a reliable, cheap and fast measurement device for the 100 kW dual fluidized bed gasification reactor at TU Wien. When the possible technologies were identified, a test-run of the plant was performed to test some of these technologies. Also, a bibliographical research was done to develop experiments for fly char activation to activated carbon. The experiments were carried out in a cylindrical quartz fluidized bed reactor at TU Wien and the product was analyzed in a surface area and porosity analyzer.

The results obtained from the test-run were not as expected, because the measurements did not match previous results. This can be solved in future attempts by improving the sampling or recalibrating the analyzers. With regard to the external physical activation of fly char, with the selected parameters the carbon content was removed from the sample within a retention time of 2 hours. During the experiments, a reduction of the sample mass was observed, meaning that new pores were created and the existing ones were narrowed. Nevertheless, this observation requires to be validated with a BET and porosity analysis.

The outcome of the master thesis is a literature study comparing the most recommended measurement technologies for sulfur (H₂S, COS) and nitrogen (NH₃, HCN) impurities found in product gases from gasification processes. Besides, the possibility of an external physical activation was explored. Further research should be done finding the proper implementation of the recommended measurement technologies and to find suitable measurement technologies for tar impurities. Additionally, the porosity and the surface area from the resulting upgraded fly char should be analyzed and the physical activation should be performed in a bigger reactor to be able to use recommended gas flowrate values and to avoid the delay in the measurement systems due to the low gas flowrate. Furthermore, the physical activation process should be optimised performing experiments for multiple retention times to improve the quality of the product.

Acknowledgements

The results presented in this thesis are part of the project ReGas4Industry (871732) funded by the Austrian Climate and Energy Fund supported by the Austrian Research Promotion Agency (FFG). The work has been accomplished in cooperation with BEST Bioenergy and Sustainable Technologies GmbH.



Table of contents

1	INTRODUCTION	1
2	STATE OF THE ART OF BIOMASS GASIFICATION AND GAS CLEANING	3
2.1	BIOMASS UTILIZATION IN DFB STEAM GASIFICATION	3
2.2	DUAL FLUIDIZED BED OVERVIEW	5
2.2.1	Principle of methanation	8
2.2.2	Principle of Fischer-Tropsch synthesis	8
2.3	GAS COMPOSITION AND SPECIFICATION OF THE CATALYSTS	10
2.4	SULFUR COMPOUNDS MEASUREMENT	13
2.4.1	Gas Chromatography (GC)	13
	Principle of Mass Spectrometry Detector (MSD)	15
	Principle of Thermal Conductivity Detector (TCD)	15
	Principle of Flame Photometric Detector (FPD)	16
	Principle of Pulsed Flame Photometric Detector (PFPD)	17
	Principle of Sulfur Chemiluminescence Detector (SCD)	18
	Principle of Photoionization Detector (PID)	19
	Principle of Electrolytic Capture Detector (ELCD)	20
	Principle of Atomic Emission Detector (AED)	21
	Principle of Barrier Ionization Discharge (BID)	22
2.4.2	Principle of Tunable Diode Laser Absorption Spectroscopy (TDLAS)	23
2.4.3	Principle of Quantum Cascade Laser (QCL)	23
2.4.4	Principle of Fourier-transform Infrared Spectroscopy (FTIR)	24
2.4.5	Principle of Non-Dispersive Infrared (NDIR) Analyzer Module	25
2.4.6	Principle of Ultraviolet–Visible (UV-VIS) Absorption Spectroscopy	26
2.5	NITROGEN COMPOUNDS MEASUREMENT	27
2.5.1	Principle of Nitrogen Chemiluminescence Detector (NCD)	27
2.5.2	Principle of Nitrogen-Phosphorus Detector (NPD)	28
2.6	TAR MEASUREMENT	29
2.6.1	Tar Guideline (TU Wien)	29
2.6.2	Flame Ionization Detector (FID)	30
2.6.3	Continuous Tar (CON-TAR) Analyzer	31
2.6.4	Molecular Beam Mass Spectrometry (MBMS)	31
2.7	GAS CLEANING	33
2.7.1	Tar removal	34
2.7.2	Sulfur removal and recovery	35
2.7.3	Nitrogen removal	37
2.8	FLY CHAR FOR GAS CLEANING	38
2.8.1	Synthesis of AC	39

2.8.2	<i>Gas cleaning processes</i>	40
2.8.3	<i>Influence of ashes on char reactivity</i>	42
3	EXPERIMENTAL SETUP OF FLY CHAR TESTING	43
3.1	DESCRIPTION OF THE TEST PLANT.....	43
3.2	EXPERIMENTAL PROCEDURE	46
4	RESULTS	48
4.1	RESULTS FROM EXPERIMENTS	48
4.2	PROPER CHOICE FOR MEASUREMENT DEVICE.....	52
4.2.1	<i>Sulfur impurities measurement</i>	53
4.2.2	<i>Nitrogen impurities measurement</i>	57
5	CONCLUSION AND OUTLOOK	60
6	NOTATION	64
	SYMBOLS.....	64
	ABBREVIATIONS	65
7	LIST OF TABLES	68
8	LIST OF FIGURES	69
9	REFERENCES	71

1 Introduction

Climate change is one of the most pressing issues of our time. Its effects are unequivocal and, since the 1950s, many of the observed changes are unprecedented over decades to millennia. The atmosphere and oceans have warmed, the amounts of snow and ice have diminished, and the sea level has risen. This phenomenon has been caused mainly by human influence due to the increasing anthropogenic emissions of greenhouse gases (GHG) [1].

The European Union signed the Paris Agreement, which was adopted by consensus in 2016. This agreement aims to mitigate global warming and states that countries have to pursue efforts to limit the temperature increase to 1.5 °C above pre-industrial levels, recognizing that this would significantly reduce the risks and impacts of climate change [2].

To successfully achieve the Paris Agreement aims, there should be a change in how modern societies produce energy and complex organic carbon compounds. The U.S. Energy Information Administration states that 5,268 million metric tons of energy-related CO₂ were emitted to the atmosphere by the United States because of fossil fuels consumption in 2018. As seen in **Figure 1**, the amount of CO₂ emitted each year from fossil fuels, cement and flaring tends to increase. Without any mitigation strategies, computational models predict that the global temperature change for the end of the 21st century will likely exceed 2 °C. This rise will have a large negative impact on the most sensitive continents such as Africa [1].

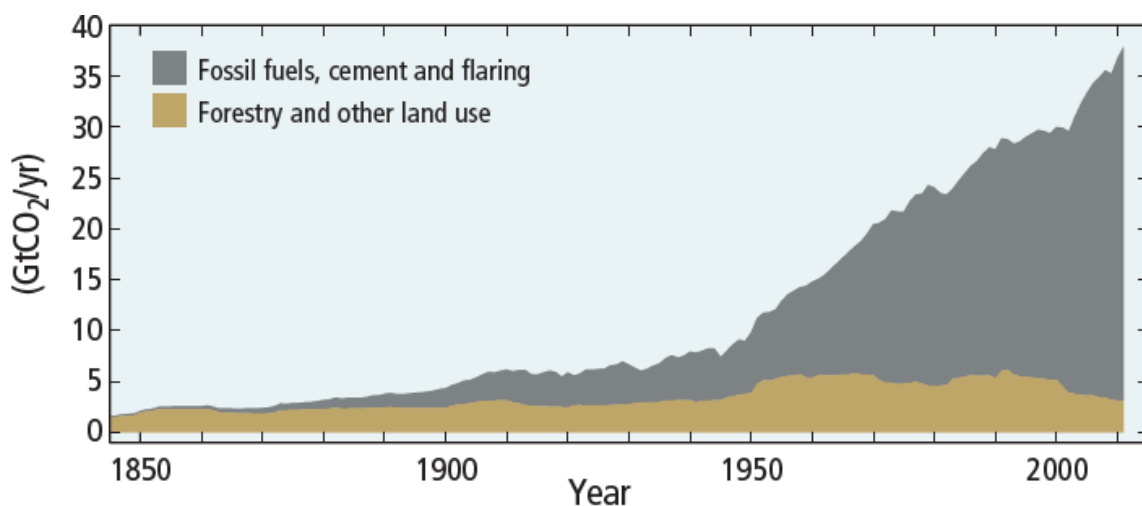


Figure 1: Global anthropogenic CO₂ emissions from the most CO₂-intensive human activities [1].

One of the targets of the European Union to mitigate global warming is to increase the share of renewable energy in the final energy consumption to 32% by 2030. Data from 2018 reveals that the share of renewable energy at that time was 18.9% [18]. Another objective is to reduce GHG by at least

40% by 2030 compared with 1990 levels. The last results from 2018 showed that the GHG emissions across the EU had fallen by 23 % compared with 1990 levels [3]. A technological development in biofuels and biomass energy production can have a huge impact on the mitigation of climate change effects and, therefore, contribute to meet the 2030 objectives.

Compared to fossil fuel biomass is a renewable fuel making it more environmentally friendly. It can be obtained from different sources. The main technologies for the conversion of woody biomass are pyrolysis, combustion and gasification. This work focuses on the gasification technologies. Gasification is performed at TU Wien in an advanced Dual Fluidized Bed (DFB) gasifier. Nowadays, conventional biomass cannot compete economically with fossil fuels. Hence, the latest design of the DFB gasifier was designed for the purpose of utilizing inexpensive fuels such as municipal residues. [4]

The use of residues in gasification implies a technological challenge not only on the gasification reactor but also on the cleaning process due to the high content of different impurities. Ultra-clean syngas is required to avoid catalyst poisoning in the upgrade process to acquire a high valuable final product. For this reason, the deployment and implementation of inexpensive yet accurate gas analysis techniques to monitor the fate of gas impurities might play an important role in the commercialization of biomass and waste gasification processes. [47]

To make the process more economically competitive, creative ways for the valorisation of the by-products have to be developed. Fly char is one of the multiple by-products from gasification. Normally, fly char is sold to the agriculture sector [21]. However, when using olivine as bed material, the fly char contains a high amount of heavy metals and therefore cannot be used in agricultural applications.

A different application for fly char is the utilization as adsorbent for gas cleaning processes. The replacement of cold gas cleaning methods such as wet scrubbers with an activated carbon guard using upgraded fly char could lead to a big decrease of the price because these cleaning methods are more efficient and the adsorbent is a by-product from the process [20].

The aims of the present work are to find the most suitable measurement technology to measure nitrogen and sulfur impurities. The technology should be reliable, cheap and fast when measuring nitrogen and sulfur impurities. Furthermore, an experimental work to evaluate the use of fly char as an adsorbent in the gas cleaning process was carried out.

2 State of the art of biomass gasification and gas cleaning

The gasification of solid materials is not a new technology. It was discovered during the late 1700s and early 1800s to produce tar. During the last 20 years, gasification technologies started to flourish, trying to become an efficient source of energy output using renewable resources [53].

Gasification can be briefly defined as the thermochemical conversion of a solid or liquid carbon-based material (feedstock) into a combustible gaseous product (combustible gas) by the supply of a gasification agent (another gaseous compound) [54]. The following chapters describe the state of the art of the gasification technology and deal with the most important aspects such as the reactor design, operational conditions, cleaning steps and gas measurement devices.

2.1 Biomass utilization in DFB steam gasification

Gasification processes mostly use woody biomass to create a wide range of products. Nevertheless, these resources are expensive and it was concluded that the gasification process is economically not competitive if high quality biomass resources are used as fuel [4]. With the development of the DFB gasifier from TU Wien, alternative and cheaper fuels like biogenic residues or waste from agriculture, industry, and municipalities can be used in the gasification process.

If residues or other fuel types like waste materials are used, the product gas composition will change significantly especially for tar contents and impurities. To use these competitive fuels, a complex and challenging cleaning process is required. The research of new cleaning systems and impurity measurements will contribute to make biomass gasification a cheaper system and, in the future, it could be a competitor to fossil fuels [4].

Figure 2 compares different resources and products. In this figure sewage sludge is the most difficult to process and liquid fuels and chemicals are the most difficult to produce due to technological challenges.

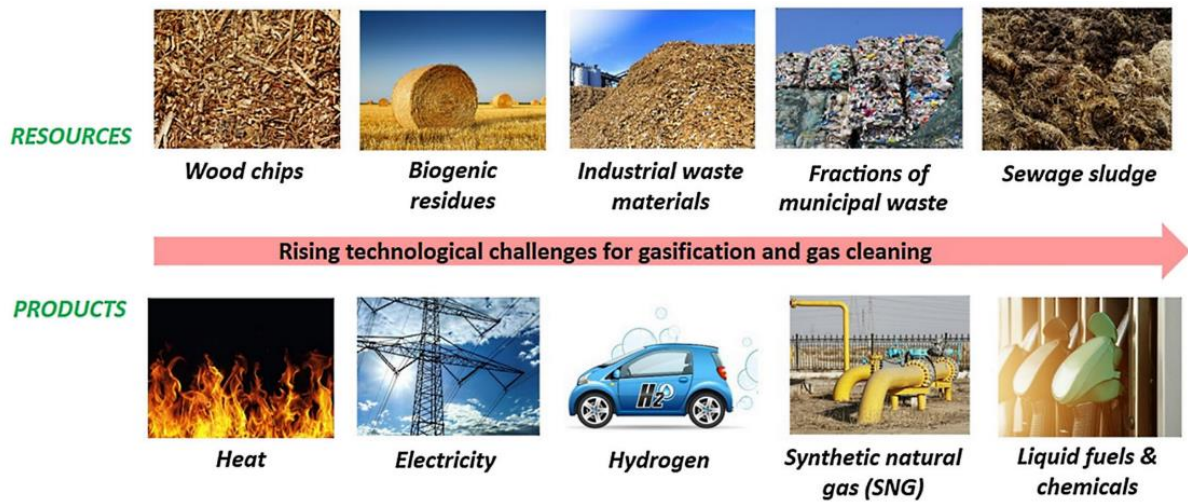


Figure 2: Future industrial applications of biomass gasification technology [4].

The main compounds of the gas produced in the gasification are H_2 , CO , CO_2 and CH_4 . The product gas can be used to generate heat or/and electricity or it can be upgraded to create products that are more valuable [4]. These applications will be further discussed in following chapters.

2.2 Dual Fluidized Bed overview

Since 1990, research in the field of gasification is ongoing at TU Wien. The first DFB reactor concepts showed good results when wood chips were used as fuel for gasification. However, this raw material is expensive and therefore not competitive against fossil fuels. A possible solution to increase the market penetration of this technology is the efficient gasification of inexpensive fuels such as sewage sludge or other residues. However, the gasification of these fuels is technologically challenging due to the poor chemical and physical properties. To cope with this challenge, TU Wien developed a novel DFB gasification reactor in 2014. With this reactor concept, biogenic residues and waste materials can be successfully used as fuel [17].

As it can be seen in **Figure 3**, the DFB process consists of two main parts: the gasification reactor (GR) and the combustion reactor (CR). The fuel input is realized in the lower part of the gasification reactor. Here, drying and devolatilization of the initial fuel and the gasification of char with the gasification agent occur at temperatures between 750-850 °C. The residual, ungasified char and the bed material are transported to the CR via loop seals. Inside the CR, the bed material is heated up by the combustion of the residual char with air. The CR reaches temperatures of 900-970 °C. The CR is designed as a fast fluidized bed, thus enabling the bed material to circulate between the two reactors. A gravity separator is used to separate the bed material from the flue gas before it is recirculated the upper part of the GR. The upper part of the GR is a counter current column, with hot bed material flowing to the lower part of the GR and product gas from the gasification of the fuel flowing upwards. Finally, the product gas is separated from the bed material and the fly char using another gravity separator [4] [17].

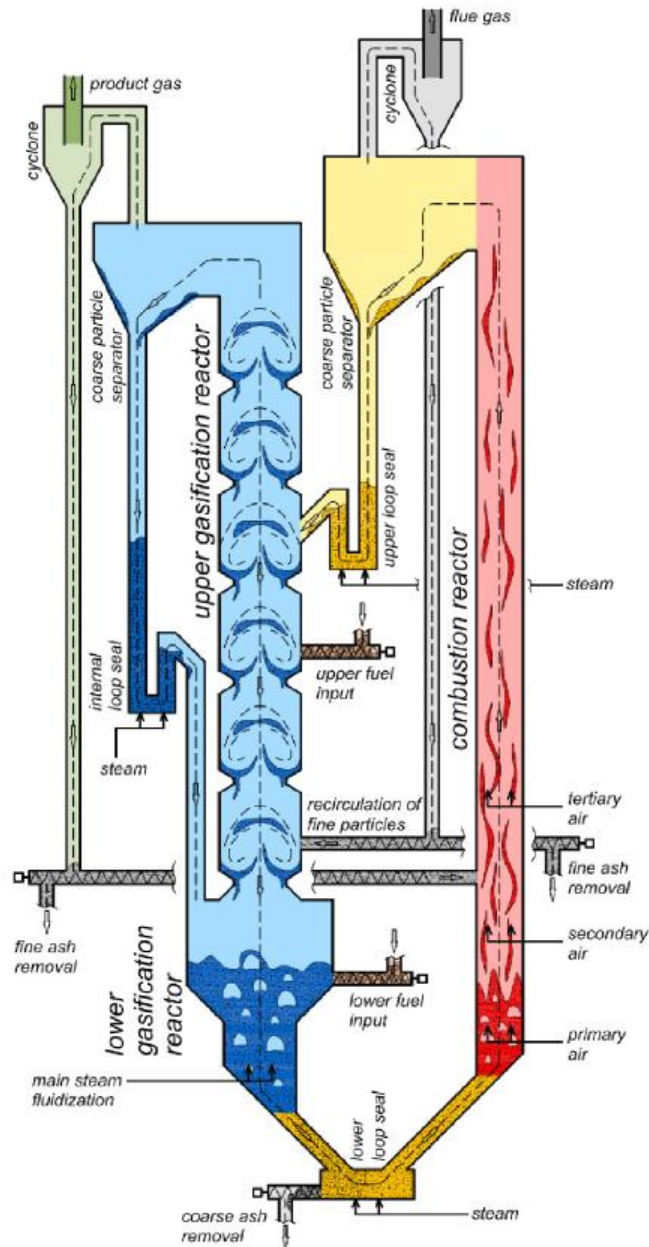


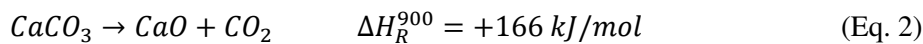
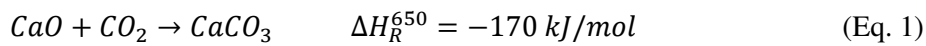
Figure 3: Schematic diagram of the DFB gasification reactor from TU Wien [17].

The selection of the gasification agent was proved to have a strong impact in the product gas composition. Experiments with steam, carbon dioxide and a mixture of both have been carried out. The results shows that the increase of the CO_2 input reduces the concentration of H_2 while the CO and CO_2 content is increased in the product gas [4].

Different bed materials can be utilized in the DFB process. The choice of the bed material is important for synthesis processes because it shows an impact on the H_2/CO ratio of the product gas. Normally, olivine is used as bed material during DFB gasification. The advantage of olivine is its catalytic activity due to the formation of calcium-rich layers on the surface of the particles during long-term operation. Nevertheless, this bed material is expensive and its availability is regionally restricted. This issue has

led to different investigations about different bed materials [4].

Sorption enhanced gasification (SEG) uses limestone or dolomite as bed material. The consequence is a selective transport of CO_2 from the GR to the CR [4]. During SEG, the produced CO_2 in the GR reacts with the bed material according to **Eq. 1**. Then, the CaCO_3 circulates to the CR via the loop seals. Due to the high temperature in the CR, the bed material returns to its original state according to **Eq. 2** and CO_2 is emitted from the CR instead of from the GR [4].



With this technique, the H_2 content in the product gas is higher with maximum values of 70-75 vol%. Besides, the H_2/CO ratio is higher and can reach values from 2 to 10 mol/mol, while the typical H_2/CO ratio for olivine is only 2 mol/mol. The H_2/CO ratio has a key role in the synthesis of the produced syngas [4].

Different products can be produced using syngas. The simplest option is the combustion of product gas for industrial heat or co-firing. In this application, the product gas is blown directly into a combustion chamber of a pulverized coal-fired power station. This allows the reduction of CO_2 emissions and an economical advantage by replacing hard coal or lignite with cheap waste fuels. Another option is the use of combined heat and power generation. In this process, the product gas has to be cleaned before it is fed into gas engines or gas turbines. The last option is to use syngas as an intermediate gas for synthetic products. Nevertheless, these synthesis processes require a considerable investment. The most common synthesis processes are the FT process, methanation, and the synthesis of mixed alcohols, methanol and dimethylether (DME). These products can be used to produce heat, electricity or can be sold for other applications [5]. **Figure 4** summarizes the different paths for syngas utilization.

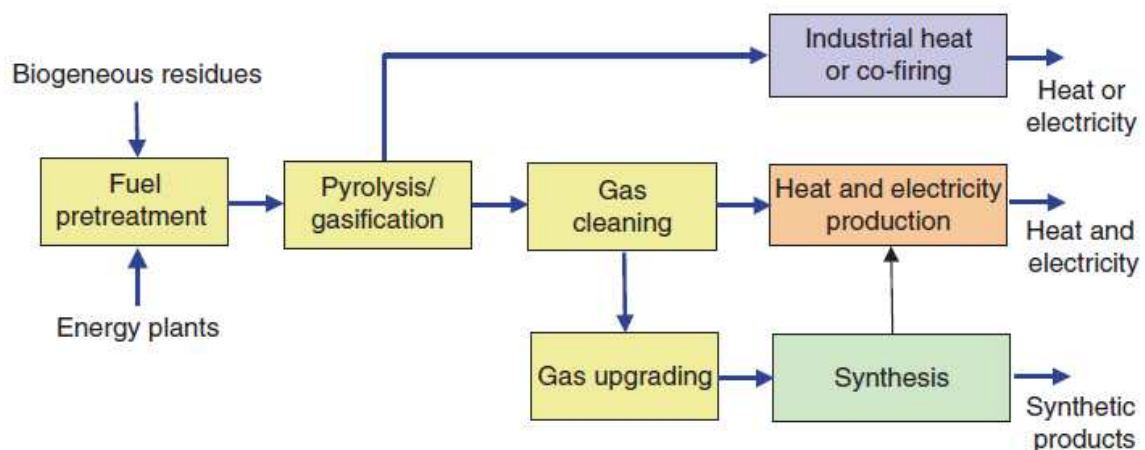


Figure 4: Different ways for syngas utilization [5].

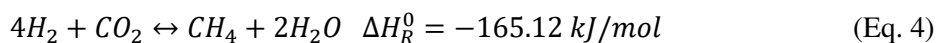
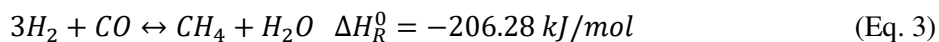
In the following chapters, methanation and FT synthesis will be detailed due to their huge importance in the industry and transport sector with regard to the other synthesis technologies.

2.2.1 Principle of methanation

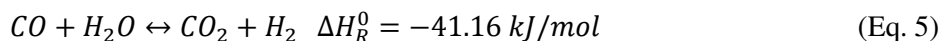
Methanation aims to maximize the conversion of carbon-containing molecule species into methane. The synthetic natural gas (SNG) produced must meet the quality requirements to be injected in the natural gas grid. SNG must have a minimum methane content of 96 mol-% in Austria. Moreover, CO has to be under 0.5 mol-% due to its toxicity and gases with low or no volumetric heating value such as nitrogen, carbon dioxide or hydrogen are allowed in a range of a few percent [14].

Production of SNG from syngas is a complex step, it requires a specific composition (e.g. H₂/CO ratio) and an ultra-clean gas. Therefore, a gas upgrading is necessary in most of the cases. Methanation has a complex mechanism of different exothermic reactions that can happen as a gas-gas interaction or as an interaction of the gas with the catalyst surface.

The main reactions are CO- and CO₂- methanation, also known as the Sabatier reaction [6]:



The water-gas shift (WGS) reaction (**Eq. 5**) is very important in this process. It can be performed inside the methanation reactor or in an upstream step to meet the stoichiometric H₂/CO ratio of 3:1 mol/mol for the methanation process. If WGS is omitted in an upstream step and a cold gas cleaning process is applied, the water content has to be adjusted by adding steam to allow for a simultaneous water gas shift reaction inside the methanation reactor [6].



Methanation is a catalytic process, so the catalyst selection has a huge importance. There are different options available, however, nickel is the most commonly applied active metal for commercial methanation applications. The reason of this is that nickel is the most selective methanation catalyst, shows a relatively high activity and is inexpensive compared to other catalysts for methanation. Al₂O₃ in the γ-modification is commonly used as catalyst support to improve the catalyst performance [24].

2.2.2 Principle of Fischer-Tropsch synthesis

In FT process, syngas is converted to hydrocarbons of different chain length such as the hydrocarbon

constituents of gasoline and diesel as well as wax, olefins, and alcohols [7]. This process is extremely flexible on what it can produce and strongly dependent upon reaction, process conditions and catalyst choice. Moreover, it is a good synthesis option when using olivine as bed material due to the required H_2/CO ratio of 2. **Figure 5** shows the five main primary reactions. These reactions lead to a wide variety of products, however, the FT-process can be optimised to be selective [8].

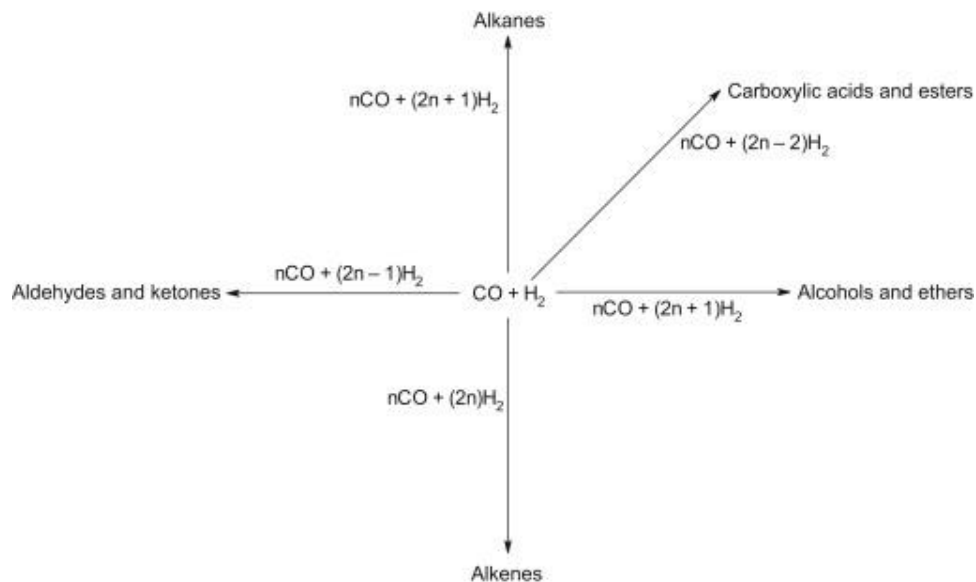


Figure 5: Path to different products via FT-synthesis [8].

Transition metals such as Fe, Co, or Ru are used as a catalyst. Among these catalysts, Ru-based types exhibit the highest activity and C_5+ selectivity. Nevertheless, Ru is an expensive material and therefore its use is limited. Although Fe is an earth-abundant transition metal, it shows a high WGS reaction activity, thus lowering C_5+ selectivity. Lastly, Co-based catalysts exhibit relatively high activity and selectivity to long-chain paraffins, high resistance to deactivation, and a low WGS reaction activity. Thus, well-dispersed Co-based catalysts supported on silica or alumina are generally preferred in FT processes [25].

2.3 Gas composition and specification of the catalysts

As explained before, synthesis processes require a catalyst to produce a valuable final product. These catalysts are usually extremely sensitive to impurities. When the impurities deactivate the catalysts, the catalysts must be reactivated again or replaced with new catalysts, increasing the variable costs of the plant. To avoid this, a cleaning process before the synthesis process is required. Nevertheless, the outlet gas composition has to be studied first in order to develop a proper cleaning system. A correct cleaning process will reduce the amount of impurities on the catalyst and avoid the catalyst deactivation.

Nitrogen from the fuel is converted mainly to NH_3 by reacting with H radicals. The amount of NH_3 in the product gas was suggested to have a linear relationship with the amount of nitrogen in the fuel composition. Remaining fuel nitrogen is converted mainly to N_2 and HCN and a minor fraction of nitrogen from the fuel is in the tar, char and in the NO emitted from the combustion reactor [9].

The main part of the sulfur in the fuel is emitted as gas, however, a minor part is bounded in char, tar and ash during thermal conversion. In gasification, most of the sulfur is released in the product gas stream to form mainly H_2S as well as COS and other organic sulfur compounds to a minor extent. The amount of sulfur in the product gas not only depends on the sulfur content in the fuel. H_2S concentration in the product gas can be affected not only by the sulfur content in the fuel, but also by the ash composition. Alkali metals and alkaline earth metals are capable of reacting with H_2S formed during devolatilization and, therefore, reduce the H_2S concentration in the product gas [9].

Within the last years, experiments on biomass gasification using a wide variety of fuels have been carried out at TU Wien. **Table 1** shows approximate values not only for the impurities but also for the main gas components. These values were measured in the 100 kW pilot plant at TU Wien before the cleaning step. It is important to remark that the data in the table contains measurement values from the classic as well as the advanced reactor design. **Table 2** gives an approximate idea of the content of impurities in the product gas of the pilot plant using various fuels and compares it with the impurity content of an industrial DFB gasifier after the coarse gas cleaning process using softwood as fuel. This table also outlines the approximate quality requirements of the product gas for different synthesis processes.

Table 1: Average values for the impurities and the main gas components in the product gas generated during gasification before the cleaning step [4, 10].

	SW ^a	BA ^b	CM ^c	BA+CM+ST ^d	SS	WW	SCR	SCB	LI
Gasification temperature (°C)	789-851	748-846	766	772	810	840-851	849	852	789
Steam/carbon ratio (g_{H2O}/g_C)	1.4	2	1.8	1.8	n.a.	n.a.	n.a.	n.a.	1.8
Bed material	Olivine/Limestone	Olivine/limestone	Feldspar + limestone	Feldspar	Olivine	Olivine	Olivine	Olivine	Olivine
NH₃ (ppmv)	55	3,300-4,600	73,200	23,900	22,700	27,000-34,000	7,357	2,850	n.m.
HCN (ppmv)	n.m.	n.m.	n.m.	400	n.m.	n.m.	n.m.	n.m.	n.m.
H₂S (ppmv)	16-23	190-275	340-390	140	5,300	210-570	319	112	n.m.
COS (ppmv)	0.1-0.7	0.3-0.7	25-61	n.m.	n.m.	n.m.	n.m.	n.m.	n.m.
Gravimetric tar (g/Nm³)^e	0.93-6	0.68-2.07	2.69	3.55	8.2	9.6-12.4	1.7	5.55	13.1
GC-MS tar (g/Nm³)^e	0.87-11.7	1.1-6.05	8.1	7.6	3.9	7.8	1	1.9	23.9
H₂ (vol %_{db})	42.6	44	40.1	44.2	39	33.5-38	45.33	37.97	40.6
CO (vol %_{db})	26.6	23.5	21.0	22.3	16.5	27-31	24.68	25.94	20.2
CO₂ (vol %_{db})	18.9	18.5	19.8	20.0	25.5	17-19	16.51	19.33	20.8
CH₄ (vol %_{db})	9.4	8	8.0	8.4	7.8	9.5-11	6.6	9.86	11.4
C₂H₄ (vol %_{db})	2	1.86	1.07	1.48	2.4	0.3-3.5	1.07	2.5	2.3

SW, softwood; BA, bark; CM, chicken manure; SS, sewage sludge pellets; WW, waste wood; SCR sugar cane residues; SCB, sugar cane bagasse; LI, lignin; ST, straw.

n.m., not measured; n.a., not available

^aMain component gases measured at 851°C with olivine as bed material. Impurities measured at 789 °C with limestone as bed material.

^bMain component gases measured at 846 °C with olivine as bed material. Impurities measured at 748 °C with limestone as bed material.

^cMain component gases measured using a composition of 90 % feldspar and 10 % limestone for the bed material.

^dFuel composition: 60% BA and 25% CM and 15% ST based on weight.

^eThe differences between these two measurements are explained in **chapter 2.7**.

Table 2: Range of the impurity contents in the product gas and overview of the N- and S- impurity limits for different synthesis processes [4, 10, 19, 93-96].

	100 kw pilot plant experiments with various fuels ^a	100 kw pilot plant experiments with softwood	Industrial DFB gasifier ^b	Catalyst specification ^c				
				Methanol	Ethanol	FT process	Hydrogen	SNG
NH₃ (ppmv)	55-34,000	55	500-1,800	<0.1-10	<1-10	<0.02-10	<1-10	<30
HCN (ppmv)	400	n.m.	5-30					
H₂S (ppmv)	16-5,300	16-23	20-190	<0.5	<1-50	<0.01	<1-50	<0.1 ^e
CO₂ (ppmv)	0.1-61	0.1-0.7	0.3-8					
Gravimetric tar (mg/Nm³)	680-13,100	930-6,000	50-300 ^f	<0.01	<0.5 ^d	<0.1-1	<2,000-5,000	<2,000-5,000
GC-MS tar (mg/Nm³)	870-23,900	870-11,700	330-4,600 ^f					

Data collected from **Table 1**.

Measured after cooling and primary gas cleaning via fabric filter and bio-diesel scrubber using soft wood as the gasification fuel and pyrolysis as bed material with a gasification temperature of 840 °C.

N- and S- impurities are also measured in ppmv, total tar value in mg/Nm³ is provided for tars.

In ppmv

For Ni-catalysts

BTEX compounds were not included in the measurement.

Unfortunately, only few data from HCN is available in **Table 1** to make the comparison with the HCN emitted in an industrial DFB gasifier.

As can be noted from **Table 2**, synthesis catalysts are very sensitive to some impurities and require a quite low amount of impurities in the syngas. Consequently, the selection of a proper measurement device is fundamental to measure the impurities in the syngas after the gas cleaning process. Parameters like the sensitivity, price, cross-sensitivity, easiness of use and technology readiness are vital for the selection of the suitable measurement device. Although there are other impurities that can deactivate the catalysts, the focus in this thesis is only on N- and S- impurities.

2.4 Sulfur compounds measurement

The main sulfur compounds from the gas phase are H_2S and COS . Thiophenes and other minor sulfur impurities are also part of the composition of the product gas [37]. However, the content of these species is very low and the focus is therefore, on the measurement of COS and H_2S . Sulfur impurities can lead to several problems for the downstream synthesis of the syngas. Therefore, it is important to have a reliable and fast measurement method for these compounds to ensure the proper function of the gasification and gas cleaning systems.

In this chapter, several techniques for sulfur measurement (H_2S and COS) will be outlined. In addition, some of them can be used not only for sulfur measurement but also for nitrogen impurities measurement, therefore, they will be mentioned in **chapter 2.6** too.

2.4.1 Gas Chromatography (GC)

GC (**Figure 8**) is an offline measurement technology that allows the separation of the components of a mixture with the purpose of obtaining information about their molecular compositions and concentration. As can be seen in **Figure 6**, the gas mixture is fed into a sample injection device [67]. In the case of gas samples, the sample introduction device is usually a gas sampling valve. The principle of the gas sampling valve is very simple. The sample gas flows through a valve loop as seen in **Figure 6**. Afterwards, the valve rotates and injects an amount of sample gas into the column of the gas chromatograph [66].

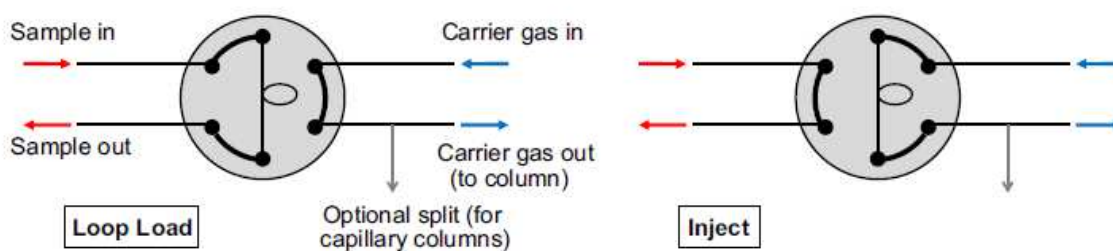


Figure 6: Example of a gas sampling valve [66].

Two different types of columns are used in a GC: packed columns and capillary columns. Packed columns have almost been replaced by capillary columns, especially by the wall coated open tubular (WCOT) capillary column. This column is made from flexible fused-silica tubing and has a microscopic layer of polymer coated in the walls of the column. This microscopic layer is known as the stationary phase. The advantages of the fused-silica are the inertness, flexibility and low price. When the sample

gas reaches the column, the gaseous compounds of the sample interact with the stationary phase. This causes each compound to elute at a different time, known as the retention time of the compound. The comparison of retention times is what gives a GC its analytical usefulness [30]. As seen in **Figure 7**, the stationary phase selected can vary depending on the chemical polarity and the polarizability of the components of the mixture [58].

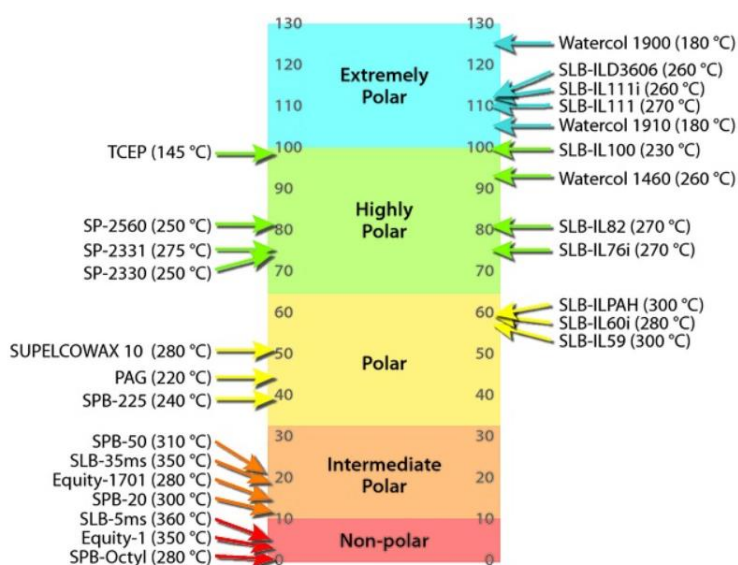


Figure 7: Most suitable stationary phases for every polarity case [58].

When the different components of the gas mixture are isolated due to the interaction with the stationary phase, the isolated components can be detected by the detector. Nevertheless, there is the possibility that the stationary phase could not isolate every component of the sample. This issue causes an overlap of the components that have the same retention time in the detector signal. However, this can be solved using a series of columns with different stationary phases [66].

The detectors can be divided in two categories: selective and universal. Universal detectors are able to detect all compounds (or most compounds) that elute. A selective detector detects only specific classes of compounds based on some molecular, elemental, or physical property. An additional important characteristic of GC detectors is their destructivity. Non-destructive detectors can detect solutes without changing them chemically. However, destructive detectors will change the solutes chemically. When the isolated compound flows through the detector, the detector will generate a voltage that is proportional to the mass of the compound or the concentration in the carrier gas of the compound. Finally, the signal is displayed by a chart recorder or/and by a computer [27].

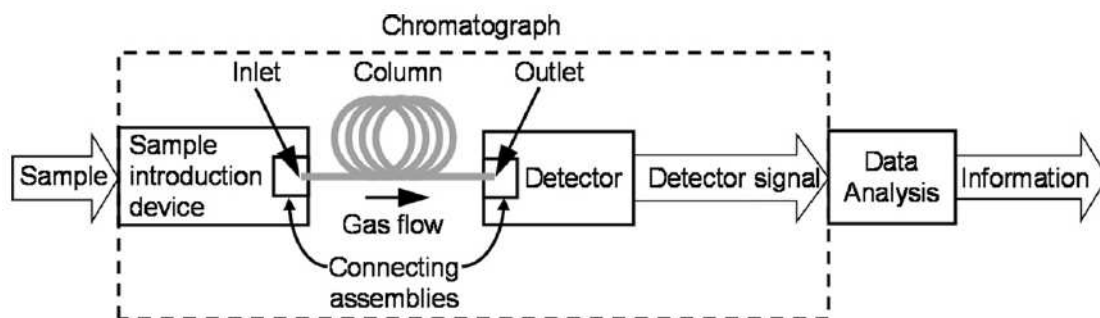


Figure 8: Block diagram of a chromatographic system [67].

Principle of Mass Spectrometry Detector (MSD)

Mass spectrometry requires the ionization of the analyte. When ions are affected by electric and magnetic fields, their velocity may increase or decrease and the direction may change. The magnitude of the deflection of the moving ion's trajectory depends on its mass-to-charge ratio. Lighter ions get deflected by the magnetic force more than heavier ions [31].

The gas chromatography-mass spectrometry (GC-MS) technique can be used for any species and allows a highly-efficient chromatographic separation and excellent limits of quantification by the use of commercial mass spectral libraries for identification of sample constituents [31]. However, it is one of the most expensive commercially available detectors and requires skilled operators for maintenance, operation and interpretation of results [47].

Principle of Thermal Conductivity Detector (TCD)

The TCD detector (**Figure 9**) consists of two electrically heated filaments in a temperature-controlled cell. When the sample is injected, the filament reduces or rises its temperature, therefore changing its resistance. A Wheatstone bridge circuit detects this change and a voltage change is produced. In most TCD designs, solutes flow directly over the filament. Some polar or reactive solutes can interact with the filaments (usually tungsten), causing the degradation of them. To minimize this, filaments are typically coated to reduce this interaction. Nevertheless, if the filaments are damaged due to the chemical interaction with the solutes, most TCD designs allow filaments to be easily replaced [29].

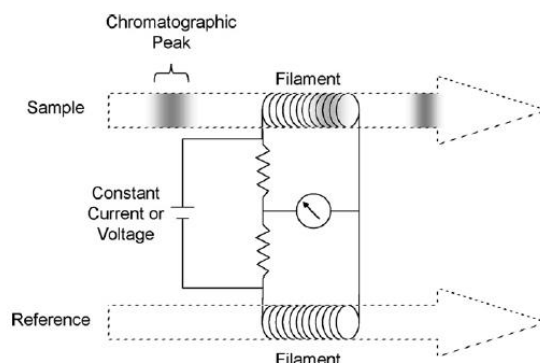


Figure 9: Schematic of a typical TCD Wheatstone Bridge [29].

The TCD is a universal and non-destructive detector that has proven over decades to be a reliable and robust GC detector, especially for the analysis of light and permanent gases. However, it is one of the least sensitive detectors [29].

Principle of Flame Photometric Detector (FPD)

In FPD (**Figure 10**), the isolated compounds eluted from the capillary column of the GC are mixed with air and H_2 and then ignited. During the combustion process of the isolated molecules in a hydrogen flame, many different forms of excited molecules are generated. When these excited ions recombine and relax into stable forms, they emit light. The spectral and temporal characteristics of the emission are specific to each species. Therefore, this effect can be used for selective detection. Finally, the emitted light is amplified by the photomultiplier tube and processed by the signal processor. High concentrations of coeluting compounds from the capillary column (as is typical when measuring sulfur in petroleum samples) can react or interact with the excited sulfur species, providing other relaxation pathways and with a different light emission. This reduces the response for a given amount of sulfur in samples compared to standards, so concentrations end up significantly under-reported. This effect is called hydrocarbon quenching [29].

The FPD is more sensitive than the TCD for the analysis of sulfur or organophosphorus containing compounds [40]. Nevertheless, the calibration and quantification using FPD is difficult due to the non-linear response [37].

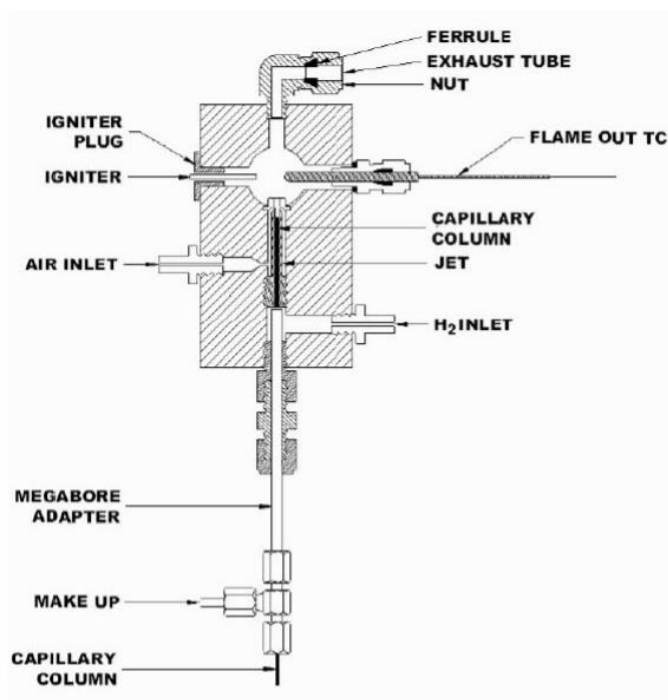


Figure 10: Flame Photometric Detector [40].

Principle of Pulsed Flame Photometric Detector (PFPD)

PFPD can be considered as an enhanced version of FPD. As seen in **Figure 11**, the detector body and part of the detector cap are filled with the wall gas (H_2) at the beginning of the process. In PFPD, the combustion gas (air) mixes with the isolated compounds eluted from the capillary column as the combustion gas fills the detector body and increases its concentration. Simultaneously, the wall gas fills the detector cap and increases its concentration. When the wall gas fills the detector cap and reaches the heated wire, it causes the H_2 to ignite. The ignition of the H_2 causes the quick depletion of the wall gas. When the flame reaches the combustion gas in the detector body, the combustion of air mixed with the isolated compounds forms excited combustion products and they begin to fluoresce for a few milliseconds after the flame has extinguished. A few tenths of a second later, the whole process repeats [29]. This mechanism improves the selectivity because there is a different delay in the emission of the wavelength of carbon (just after the ignition) and sulfur (5-25 ms after the ignition) [41, 29]. By detecting sulfur emissions after those of carbon, most of the spectral interference from carbon can be eliminated. This technology is more sensitive than FPD but requires more maintenance and more skilled operators. Furthermore, like FPD, this approach is still susceptible to hydrocarbon quenching by high concentrations of coeluting solutes but it is easier to calibrate due to the linear response [29].

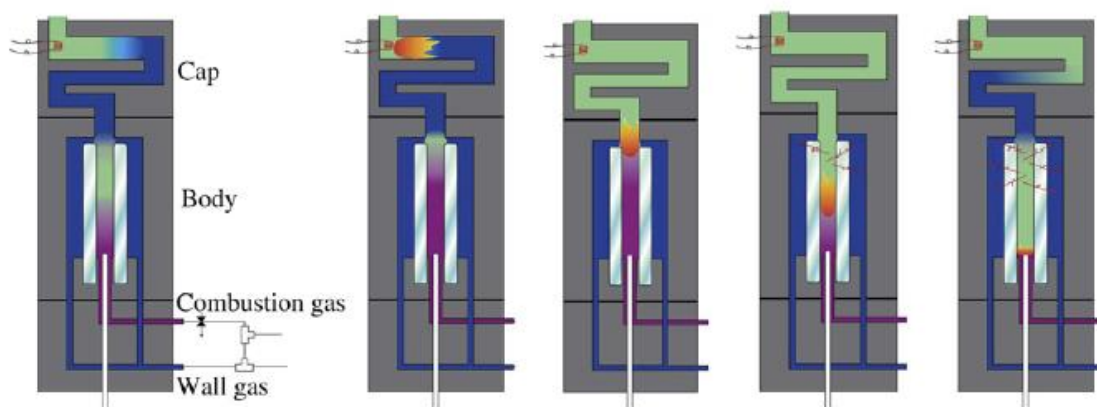


Figure 11: Detection process of a PFPD [29].

Principle of Sulfur Chemiluminescence Detector (SCD)

Gas-phase ozone-induced chemiluminescence reactions are the basis in chemiluminescence detectors (CLD). The elemental content of sulfur or nitrogen in an analytical sample can be analyzed using this mechanism. The CLD can be used for the specific detection of S (SCD) or N (nitrogen chemiluminescence detector). As seen in **Figure 12**, the previously isolated sulfur compounds (R-S) eluted from the GC column are fed into a burner. In the combustion chamber, the isolated sulfur compounds are oxidized at approximately 800 °C using air (**Eq. 6**) [29]. Conversion of sulfur appears to be complex and involves catalytic reactions on the surface of the metal oxide tubes or the container where the sulfur chemiluminescent species (generically denoted as X-S) are generated [32]. Hydrogen is added near the exit of the burner to ensure that all final combustion products are volatile, thus reducing fouling of the burner [29].



Following this step, the resulting species of **Eq. 7** are mixed with O_3 and flow through a reaction chamber. In the reaction chamber, a low-pressure reaction (<0.016 bar) of X-S with O_3 (**Eq. 7**) is performed, further oxidizing X-S until an excited SO_2^* molecule is created. As the excited SO_2^* molecule relaxes, it emits characteristic light ($h\nu$) [29][32].



The emitted light ($h\nu$) is filtered and detected by a photomultiplier tube (PMT) and then amplified, yielding a linear response relative to the mass of S [29].

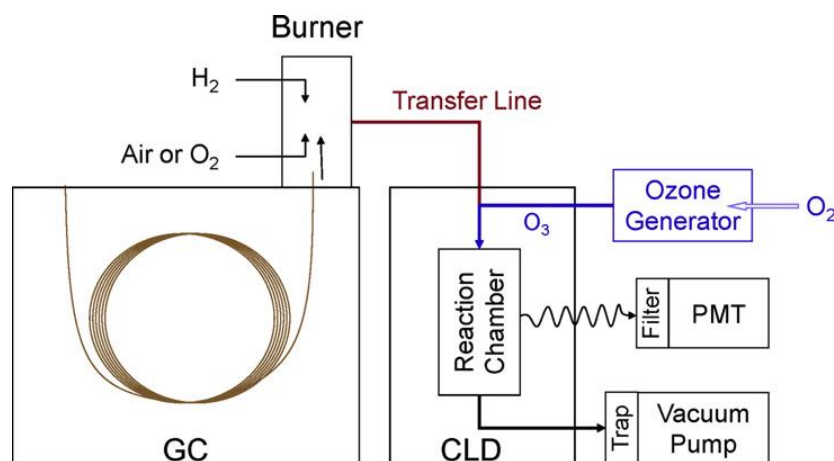


Figure 12: Block diagram of a CLD [29].

SCD is a sulfur-specific detector that can measure in the low ppb range and, unlike FPD and PFPD, it does not have hydrocarbon quenching issues. Nevertheless, it is an expensive technology and it has to be operated by a skilful operator. The maintenance of this equipment is also a very complex process but, like PFPD, it has a linear response, making the calibration process easier than the calibration of a FPD [29]. There are some molecules that interfere with the measurement: benzene and thiophene (because of coke formation in the SCD reaction tube), H₂S (which is usually several orders of magnitude higher than other sulfur compounds), and H₂ (since it can deactivate the SCD reaction tube). To prevent these interferences, a dilution of the sample is recommended (e.g. via 10:1 split) [47].

Principle of Photoionization Detector (PID)

The main part of a PID is an ultraviolet (UV) lamp filled with a gas, which emits a monochromatic radiation. If the energy of an incoming photon generated by the UV light is high enough, photo-excitation of the isolated compound carried by the carrier gas can occur, which results in positively charged molecules that generate a current directly proportional to the concentration of the compound. Choosing the correct gas to fill the UV lamp is crucial because each gas emits light in different wavelengths and, therefore, with different energy content. The selection of the gas will affect the detection of the different compounds in the sample [47]. PID are usually used to detect volatile organic compounds (VOC). However, they cannot be used to measure SO₂, N₂ and HCN [39].

As seen in **Table 3**, H₂S and NH₃ can be detected, although the relative sensitivity to these compounds is very low. For this reason, the most appropriate way to use this detector is for tar measurement. Furthermore, it is not fully commercial, a validation in different gasifiers and with different fuels is still needed [47].

Table 3: Approximate response of compound classes by PID [39].

Compound Class	Relative Sensitivity
Aromatics including Heterocycles	++++
Olefins	+++
Sulfides & Mercaptans	+++
Organic Amines	+++
Ketones	+++
Ethers	+++
Silicate Esters	+++
Organic Esters	++
Alcohols	++
Aldehydes	++
Alkanes	++
Alkyl halides	
Iodides	++++
Bromides	+++
Chlorides	+
Fluorides	-
Borate & Phosphate Esters	++
H ₂ S, NH ₃ & PH ₃	+ to ++
Organic Acids	+
Noble Gases, H ₂ , CO, CO ₂ , O ₂ , N ₂ , HCN, SO ₂ & O ₃	-
Mineral Acids	-

Principle of Electrolytic Capture Detector (ELCD)

In ELCD (**Figure 13**), the product gas carried by the carrier gas is converted to an ionizable gas using reductive conditions at temperatures from 800 to 1,100 °C in a catalytic micro reactor [29]. The ionizable gas is then carried to the detection cell, which has a continuously running flow of deionized solvent. When the ionisable gas meets the solvent, a portion of the ionizable gas dissolves into the liquid. This increases the conductivity of the mixture, which in turn is measured by two electrodes that constantly monitor the conductivity of the mixture [35]. Finally, the solvent stream flows through a deionizing resin bed and through a filter to be recycled [29]. Although the principal mode of operation of the ELCD is the halogen mode, sulfur and nitrogen modes are also available. Each detection mode requires a specific reactor, resin cartridge, and solvent.

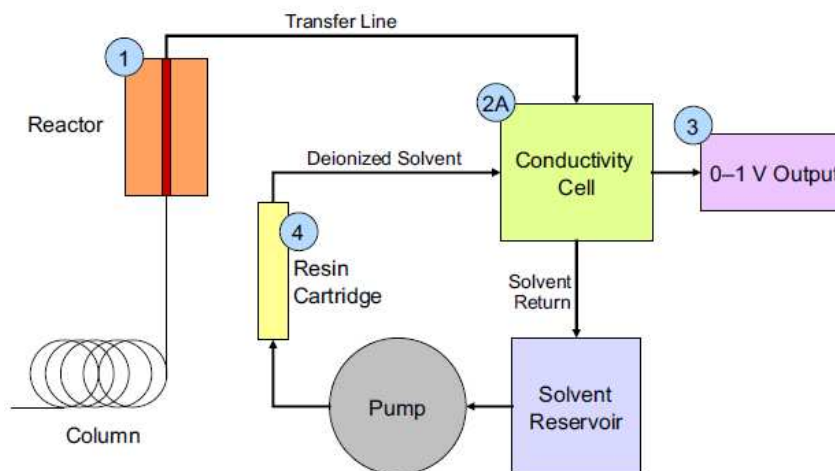
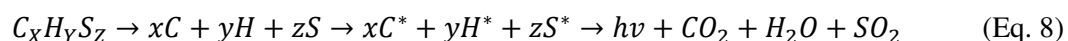


Figure 13: Schematic of an ELCD [29].

In comparison to the sulfur-selective FPD, the ELCD has lower detection limits, a linear response, and similar selectivity ratios. However, this technology also has cross-sensitivity issues with hydrocarbons, is more expensive and has a complex maintenance [79][80]. Another important disadvantage is that it has not been validated in a gasifier with different fuels [47].

Principle of Atomic Emission Detector (AED)

In AED (**Figure 14**), the separated compounds are fed into a microwave-powered plasma cavity (the plasma is usually helium). The high temperature of this plasma results in atomization of the separated compounds followed by excitation of the constituent atoms [34]. When the atoms are excited, they interact with other atoms in proximity to form stable molecules. In this process, the atom emits light at discrete wavelength ($h\nu$). Each atom has characteristic atomic emission lines. For example, in **Eq. 8**, if the eluted compound has C, H and S in its composition ($C_xH_yS_z$), when the compound is fed to the plasma cavity, the atoms from the molecule are separated and then excited. When they interact, the atoms form stable molecules (CO_2 , H_2O , SO_2) and emit light at characteristic wavelengths [29].



Finally, the emitted light is separated and detected by a purged spectrometer capable of monitoring emissions from the vacuum UV (near 150 nm) to approximately 800 nm. By spectroscopically selecting and monitoring these atomic or molecular product emission lines, one can selectively detect atoms of interest in eluting compounds [29].

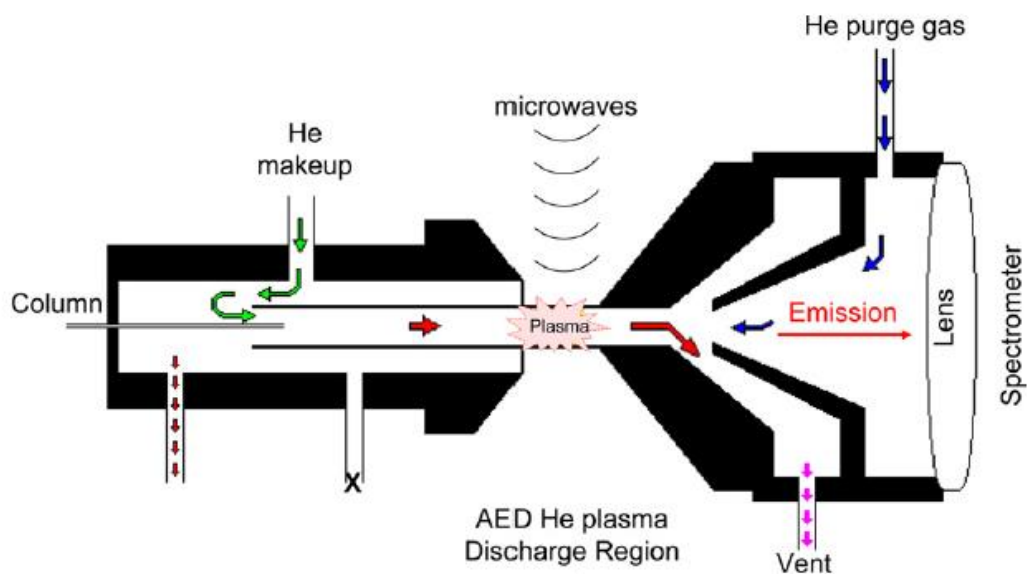


Figure 14: Detailed look at AED detection processes [29].

An AED is a very sensitive as well as selective detector in a GC and provides element-specified information on separated species. The advantage of the AED relative to other chromatographic detectors (FID, PFPD, TCD, etc.) lies in its ability to generate selective detection for every element. Thus, the AED can generate useful compositional information from gas chromatographic analytes. The limitation of AED lies in its inability to analyze non-volatile (polymeric and metal–organic salts) components and shows a somewhat inadequate selectivity and sensitivity for nitrogen and a poor baseline stability for oxygen [38]. AED has a linear response and no hydrocarbon quenching issues. However, it is more expensive than SCD and its lower detection limit is higher than the lower detection limit of a PFPD [37].

Principle of Barrier Ionization Discharge (BID)

In this detector, plasma is generated by applying a high voltage to helium in a dielectric quartz chamber. The sample from the GC is ionized by the plasma and then captured by collection electrodes. This detector is capable of measuring every compound except Ne and He, with high sensitivity [42].

The advantage of BID with regard to other detectors is that it is 100 times more sensitive than TCD and 2 times more sensitive than FID. The fact that this detector is universal is also a positive aspect [42]. However, the high sensitivity and universal response of BID detectors also have a negative side: the easy saturation of the detector, which can make peak separation difficult [47]. This disadvantage can be very problematic when measuring syngas due to its complex chemical composition.

2.4.2 Principle of Tunable Diode Laser Absorption Spectroscopy (TDLAS)

TDLAS is an online measurement technology. In TDLAS, the laser light is tuned over a small frequency range around an atomic or molecular transition of the target species. As a result, the intensity is attenuated by absorption, and the intensity of the light transmitted through the sample is recorded. In that way, the light absorbed by the atoms/molecules at the transition can be measured relative to the baseline further away from the transition, where no light is absorbed [47]. The variation in intensity is described by the Beer-Lambert Law, which is the basis for the theory of absorption spectroscopy [43]. TDLAS application is limited to the near-infrared region (wavelengths from 800 to 2,500 nm), therefore, this measurement technology can only measure compounds that absorb light in this range [47]. Consequently, TDLAS cannot detect NH_3 , HCN and COS , however, it can detect H_2S [44].

2.4.3 Principle of Quantum Cascade Laser (QCL)

QCL is an online measurement technology. In this technology, there are semiconductor devices which produce light in the mid-IR region. They are fabricated to emit light at a desired wavelength and are made to scan a spectrum using a laser chirp technique. To start the process, a QCL is pulsed with electrical energy and heats up. As the temperature increases, the wavelength of the emitted light also increases. A laser chirp lasts about one microsecond and in this time a spectrum of between one and three wavenumbers is scanned [44].

The raw detector signal is then processed to convert it into a spectrum from which the concentration of analytes can be calculated. QCLs can be chirped up to a frequency of 100 kHz, enabling many thousands of spectra to be gathered in a few seconds and processing these spectra gives a strong signal with a good signal-to-noise ratio [44].

The scanned wavelength region is selected to enable measurement of the desired analytes and it is often possible to detect more than one compound with a single QCL device. An advanced signal processing procedure enables real time validation of measurements and greatly reduces the need for calibrations [44].

As shown in **Figure 15**, QCL systems can measure compounds that absorb light in the mid-infrared spectral region.

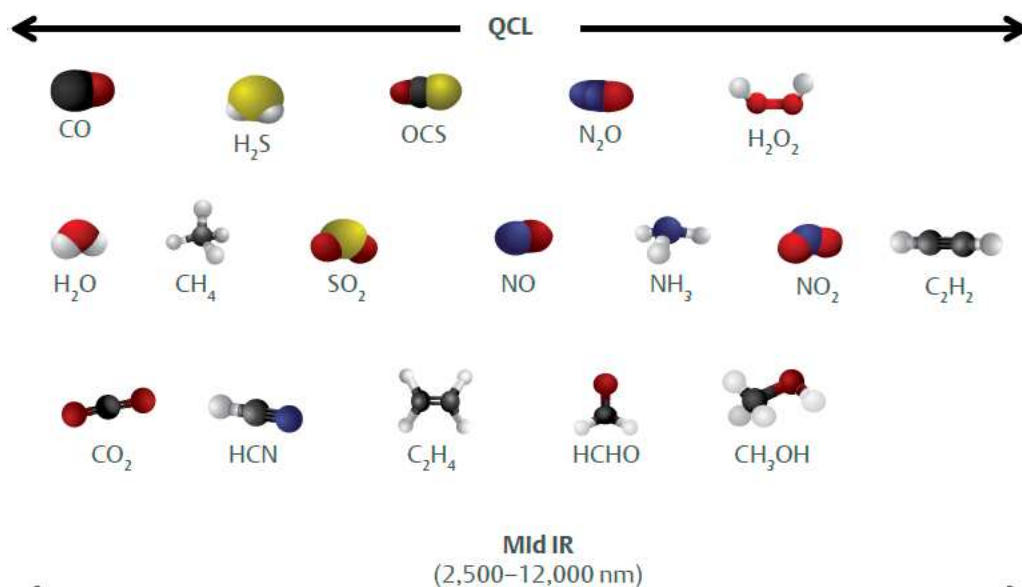


Figure 15: Compounds measured by the QCL system. [44]

TDLAS and QCL can be coupled providing greater insight and monitoring in both the near and mid-infrared range of spectroscopic light. Each QCL system can measure a specific number of compounds and it needs to be calibrated to measure these specific compounds. This detector is still not widely used and it is not a mature technology. Besides, the calibration of the detector for each compound requires a skilful operator and the detector can only measure in the low ppm range (> 0.1 ppmv) [44].

2.4.4 Principle of Fourier-transform Infrared Spectroscopy (FTIR)

The range of the infrared light is between $12,800 \sim 10 \text{ cm}^{-1}$ and can be divided into the near-infrared region, mid-infrared region and far-infrared region. The absorption radiation of most organic compounds and inorganic ions is within $400 \sim 4,000 \text{ cm}^{-1}$ [48].

A common FTIR spectrometer (**Figure 16**) consists of a source, interferometer, sample compartment, detector, amplifier, A/D convertor, and a computer [48]. The source generates radiation which passes through the product gas. A specific compound from the product gas, selectively absorbs part of the radiation, which is corresponding to specific wavelengths. The number of absorption peaks is related to the number of vibrational freedom of the molecule, whereas the intensity of absorption peaks is related to the change of dipole moment and the possibility of the transition of energy levels [47]. After irradiating the sample, the signal is amplified and converted to a digital signal by the amplifier and A/D converter, respectively [48]. Eventually, the signal is transferred to a digital computer and it performs a Fourier transformation of the interferogram yielding the spectrum of the sample [33]. The interferometer is the key component of the FTIR, and it produces a signal which encodes all the IR frequencies [47]. This means that FTIR devices can measure all wavelengths simultaneously instead of sequentially

stepping from wavelength to wavelength, thus reducing the scan time with respect to dispersive IR techniques [33].

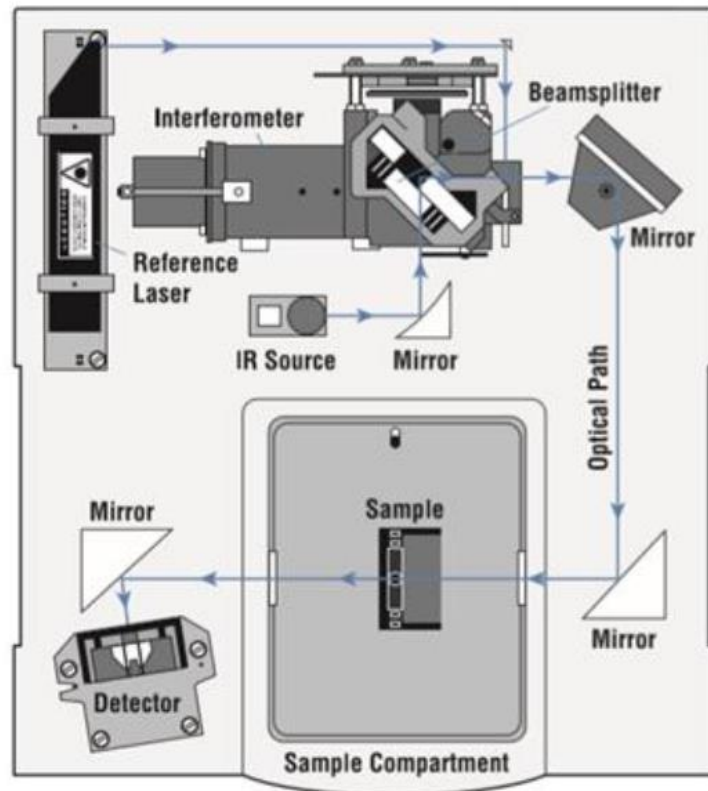


Figure 16: Simplified layout of an FTIR spectrometer [47].

FTIR is a fast and cheap technology that can be used to measure NH_3 , HCN , H_2S and COS . However, this measurements are affected by a high concentration of tar and when there is a high concentration of CO_2 and H_2O [47].

2.4.5 Principle of Non-Dispersive Infrared (NDIR) Analyzer Module

In a NDIR analyzer module (Figure 17), the infrared radiation produced by the infrared sourced is divided in two equal-energy beams. One of the beams flows through a reference cell filled with N_2 , while the other beam is mechanically modulated by a chopper and directed through the sample cell. The sample gas flows through the sample cell and adsorbs a portion of the infrared radiation. The detector converts the difference in energy between sample and reference cells to a capacitance change. This change, which is proportional to component concentration, is processed and expressed as the primary variable on the computer [47,70].

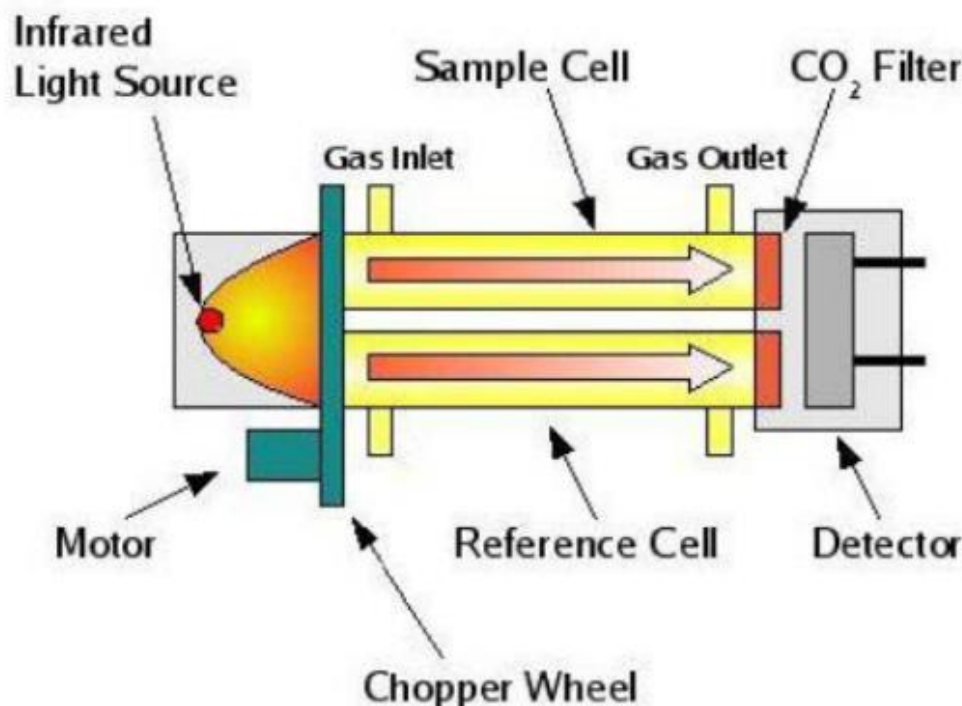


Figure 17: Schematic of a NDIR Analyzer Module [89].

The main disadvantage of this technology is the very high lower detection limit (200 ppmv), which makes it non-viable for this application [47].

2.4.6 Principle of Ultraviolet–Visible (UV-VIS) Absorption Spectroscopy

UV-VIS systems usually have a light source, a sample holder and a detector [74]. The typical UV-VIS light sources are a deuterium lamp that produces light from 170–375 nm (UV) and a tungsten filament lamp which produces light from 350–2,500 nm (VIS) [71]. The beam of light emitted by the light source is directed through the sample holder. The atoms from the sample holder absorb the light of an incident photon, exciting an electron from the ground energy state to a higher energy state. The frequency of the light absorbed is specific to the elements present in the sample and the amount of light absorbed is proportional to the concentration [73]. Finally, a diode array detector allows the instrument to simultaneously detect the absorbance at all wavelengths [74]. The concentration of an analyte in the solution can be determined by measuring the absorbance at a particular wavelength and applying the Beer–Lambert Law [72]. Sulfur compounds can strongly absorb UV radiation. This property has been applied for the measurement of H₂S, COS, CS₂ and SO₂ (the latter being a broad application of UV analyzers) [47].

The high number of different compounds present on the syngas composition makes the measurement of individual compounds difficult. Due to that, the sample has to be decomposed in a vertical oven at 1,000–

1,100°C in 2 stages, namely pyrolysis in an argon stream followed by thermal oxidation of the pyrolysis gases. All the organic S species are oxidized to SO₂, which in turn absorbs light in the UV region around 190-230 nm [47].

2.5 Nitrogen compounds measurement

In this chapter, different possibilities for measuring nitrogen compounds are described. Due to the fact that there are some systems that can detect sulfur and nitrogen compounds, the following list mentions the devices that have been described in **chapter 2.5** for sulfur measurements and can be used to measure nitrogen species as well.

- Thermal Conductivity Detector
- Mass Spectrometry Detector
- Photoionization Detector
- Electrolytic Capture Detector
- Atomic Emission Detector
- Barrier Ionization Discharge
- Tunable Diode Laser Absorption Spectroscopy
- Quantum Cascade Laser
- Fourier-transform Infrared Spectroscopy
- Non-Dispersive Infrared Analyzer Module

The next detectors described can only measure nitrogen compounds. These detectors are paired with a gas chromatographer because they need to have a system before to separate gas compounds to efficiently measure complex gas mixtures.

2.5.1 Principle of Nitrogen Chemiluminescence Detector (NCD)

The NCD mechanism is very similar to the mechanism of a SCD. The previously isolated nitrogen compounds (R-N) are fed into a burner. In the combustion chamber, the isolated nitrogen compound is oxidized at approximately 925 °C using pure oxygen and forms NO, CO₂ and H₂O following **Eq. 9**. Hydrogen is added near the exit of the burner to ensure that all final combustion products are volatile, reducing fouling of the burner [29].



Following this step, the resulting species of **Eq. 10** are mixed with O₃ and flow through a reaction chamber. In the reaction chamber, a low-pressure (<0.016 bar) reaction of NO with O₃ (**Eq. 10**) is performed, further oxidizing NO until an excited NO₂^{*} molecule is created. As the excited NO₂^{*} molecule relax, it emits characteristic light (*hν*) [29][32].



The emitted light ($h\nu$) is filtered and detected by a photomultiplier tube (PMT) and amplified, yielding linear response relative to the mass of N [29].

NCD is a nitrogen-specific detector that can measure in the low ppb range with a very good short-term and long-term precision. However, like the SCD, this technology is expensive and requires a skilled operator [81]. In this technology, the effect of CO chemiluminescence is seen to be relatively small for CO concentrations less than 10%, however, at higher CO concentrations the interference output signal grows rapidly. Moreover, when measuring large concentrations of CO₂, H₂O, O₂, H₂, or Ar, proper corrections have to be applied in the calibration method [69].

2.5.2 Principle of Nitrogen-Phosphorus Detector (NPD)

This detector consists of an electrically heated ceramic bead containing a rubidium salt, over which column effluent mixed with hydrogen and air is passed. A ‘low temperature plasma’ is generated and rubidium ions combining with nitrogen or phosphorous containing pyrolysis products leads to increased electrical conductivity, which is monitored. The selectivity for organic compounds containing nitrogen compared to organic compounds not containing nitrogen or phosphorus is about 50:1 or more. This selectivity is a major advantage for the determination of nitrogen-containing compounds in complex mixtures, since co-eluting substances not containing nitrogen or phosphorus do not interfere unless their concentrations are much higher than those of the analytes [36]. Although NPD is a sensitive detector and can measure phosphorous, it requires a higher level of instrument maintenance and is less accurate than the NCD [81]. Furthermore, the use of NPD for measuring the syngas of a gasifier has not been validated yet [47].

2.6 Tar measurement

Tar can be defined, according to the CEN/TS 15439, as the hydrocarbons larger than benzene. Having these compounds in the product gas can lead to problems of fouling and unwanted plant stops because they can condense at relevant temperatures in overall gasification processes [37].

2.6.1 Tar Guideline (TU Wien)

The most common method for tar measurement is the "tar guideline". This method uses an offline measuring setup consisting of six impinger bottles filled with a solvent. The impinger bottles are located in a cooling bath of a cryostat with a temperature of -8 °C. In the pilot plant at TU Wien, the used solvent is toluene. As detailed in **Figure 18**, the product gas is pumped through a cyclone and then through a wool-filled filter cartridge. Trace heating maintains the temperature of the gas. Downstream of the filter cartridge, the gas flows through the impinger bottles over a certain amount of time. After sampling, the solvent is filtered due to the possible contamination with particles. The particles from solvent, cyclone and filter are gathered together and dried in an oven at 105 °C for six hours. The next step is to weigh the sample and then place it in a Soxhlet extractor to remove condensed tar from the particles with 400 mL isopropanol as solvent. After the extraction, a sample of 10 mL is collected and measured with a GC-MS. Additionally the toluene from the impinge bottles is gathered together and a sample of 10 mL is collected and measured with a GC-MS. GC-MS will determine the concentration of single tar components, during the document, this measurement is referred as "GC-MS tar" [55].

This is not the only measurement done by TU Wien, the solvent phase of the Soxhlet extraction and the toluene from the impinger bottles are put separately in a rotary evaporator at 60 °C and 80 mbar. Following this, they are dried at 105 °C for another six hours. This will evaporate toluene and other light tar components, the remaining liquid is weighted and the result is the gravimetric tar. The need of two different measurements is due to GC-MS cannot measure heavy tar components and the gravimetric tar value does not consider certain light tar components. Total tar measurement cannot be obtained from the sum of these two measurement methods because some components are measured in both analysis [55].

Although isopropanol is used as solvent in the tar protocol, TU Wien uses toluene due to it has generally higher solubility for tar and the water content in the product gas can be measured simultaneously. Nevertheless, with this setup it is impossible to measure toluene [55].

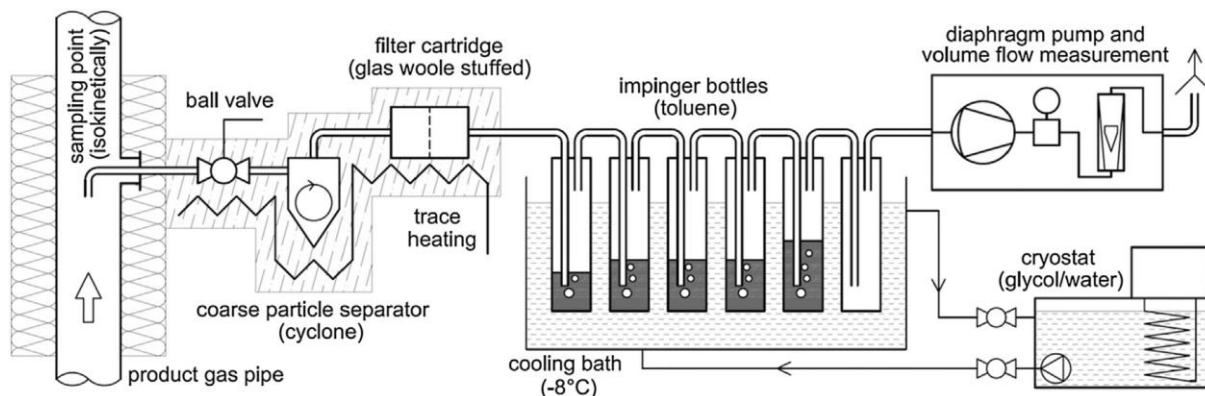


Figure 18: Schematics of the tar sampling method in the pilot plant from TU Wien [55].

Offline techniques for tar measurement are costly, cumbersome and time consuming. As a result, the development of new online measurement technologies could play a major role in the future of tar measurement [55].

2.6.2 Flame Ionization Detector (FID)

The online measurement of tar compounds can be performed on a gas chromatographer coupled with a FID. In FID (**Figure 19**), a stream of H_2 (sometimes H_2 mixed with N_2 or He) and a stream of air enter at the bottom of the FID jet and mix with the capillary column effluent prior to exiting the jet. With the help of an ignitor, a hydrogen/air flame is established above the jet [29]. In this process, ions and free electrons are formed. The charged particles produce a current flow in the gap between two electrodes located in the detector. The signal differential between the resulting current flow from the combustion of the sample and the signal from the carrier gas and the fuel gas flame provides information about the composition of the sample [47]. FID is a fast and commercially available online measurement technology that has been proved to measure tar content in gas between 200 and 20,000 mg/m^3 . Nevertheless, operational parameters such as temperature and flow range has must stay constant during the analysis.

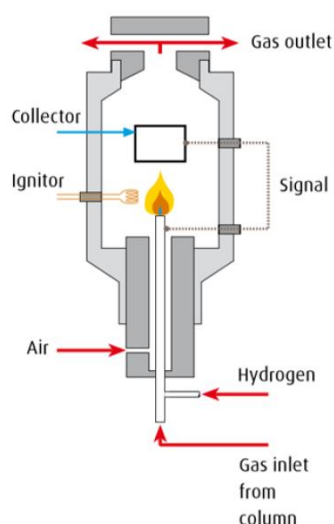


Figure 19: General diagram of a FID [47].

2.6.3 Continuous Tar (CON-TAR) Analyzer

The CON-TAR analyzer is an online measurement technology based on light induced fluorescence, by using a light emitting diode (LED) that emits UV light through an optical window into the sampling line. The properties of the polyaromatic compounds make them appropriate to get excited by the UV-light, which enables analysis of the resulting fluorescence light from these compounds. The prototype of the CON-TAR analyzer can be found in the GoBiGas plant [76]. CON-TAR analyzers are still prototypes and it is expected to have a low price for future industrial applications. In this technology, there is a limited number of tar components that can be excited at a single wavelength, therefore, there is a loss of information (semi-quantitative results). Moreover, it needs to be calibrated and the tar composition has to be known to translate the absorbance to tar concentration (more than one tar species absorb at the same wavelength) [47].

2.6.4 Molecular Beam Mass Spectrometry (MBMS)

MBMS is an online measurement technology that can be used to measure the inorganic compounds or the tar content of a sample. In this technology, a molecular beam is formed as the sample gas is drawn through a 300 μm diameter orifice into the first of the three stages of a vacuum system. This free-jet expansion results in an abrupt transition to collisionless flow that avoids chemical reactions and inhibits condensation by rapidly decreasing the internal energy of the sampled gases. The result is that the analyte is preserved in its original state, allowing light gases to be sampled simultaneously with heavier, condensable, and reactive species. The central core of this expansion is extracted with a conical skimmer, located at the entrance of the second stage. Finally, the molecular beam continues into the third stage of the vacuum system. There, components of the molecular beam are ionized using low energy electron ionization before passing through a mass spectrometer [77]. The chemical fingerprint is

instantaneously analyzed by the mass spectrometer. This online measurement technology is commercially available and can measure tar concentrations above 1 ppmv. However, it is very expensive (~ \$300,000) and is a very complex system [47].

2.7 Gas Cleaning

As described previously, the measurement system analyze the concentration not only after the gas leaves the gasification reactor, but also after the cleaning step to confirm that the syngas is ready to be synthetized. Parameters of the gas cleaning steps are varied and they must be thoroughly selected to achieve the gas quality required for the final application. This chapter will focus only on nitrogen, sulfur and tar removal. Moreover, a novel application using the fly char produced during the gasification process in the cleaning process will be introduced.

Syngas produced in a gasification process contains undesirable gas components like acid gases, etc. besides other impurities such as tars and particulate matter. Gas cleaning technologies are divided in 3 groups: Cold gas cleaning, warm gas cleaning and hot gas cleaning [14]. Each of these groups have different operational parameters and their own advantages and disadvantages. **Table 4** provides basic information about these cleaning technologies.

Table 4: Comparison between cold, warm and hot gas cleaning technologies [14].

	Operational temperature	Advantages	Disadvantages
Cold gas cleaning	Ambient temperature and below	<ul style="list-style-type: none"> Well developed and widely used 	<ul style="list-style-type: none"> Cooling units necessary Spent washing liquids need to be regenerated
Warm gas cleaning	100 - 400 °C	<ul style="list-style-type: none"> In operation at small pilot scale Hot gas filtration possible 	<ul style="list-style-type: none"> Heating and/or cooling units necessary No commercial use till now Possible catalyst poisoning
Hot gas cleaning	Above 400 °C	<ul style="list-style-type: none"> No heating or cooling should be necessary 	<ul style="list-style-type: none"> Temperature resistance of the materials is a problem No commercial use till now Possible catalyst poisoning

Overall, the need of a cleaning process for the syngas generates a high impact on the economic efficiency of this process. Some of these processes require high pressure to properly remove the impurities, therefore, the use of a compressor is mandatory in high-pressure cleaning processes because the DFB gasification is performed in atmospheric conditions. Using a compressor without firstly removing tar components from the syngas could lead to the malfunction of the compressor due to tar condensation. For this reason, a previous study of the gas components must be done in order to correctly design the steps of the cleaning process [4].

The following chapters will describe conventional methods for tar, sulfur and nitrogen impurities removal. Moreover, in **chapter 2.9**, the idea of using fly char obtained as a by-product from the DFB gasification reactor will be introduced. The removal of impurities with fly char is currently under development but maybe in the near future, it could be a competitor of the conventional tar, sulfur and nitrogen removal methods.

2.7.1 Tar removal

Tar removal methods can be structured in two types, inside the gasifier (primary method) or after the gasifier (secondary method). The choice will depend on the final application of the syngas, using a primary method, a secondary method or a combination of both [26].

Tar contents can be reduced inside the gasifier by a proper selection of operating parameters (especially temperature, gasification medium, steam to fuel ratio and residence time). The addition of active bed materials is also effective for reducing tar content in the product gas of the gasification reactor [26].

Secondary methods offer different possibilities for tar removal. Thermal cracking and catalytic cracking belong to the hot gas cleaning methods group. They use high temperature to decompose large organic compounds into small non-condensable gases [27].

Another option is using an oil-based gas washing process (OLGA). The product gas is cooled from typically 700–900 °C to the OLGA inlet temperature of 450 °C. Upstream OLGA, coarse solids are separated via cyclones. OLGA removes fine solid aerosols. In OLGA, the tars are separated, first by condensation of heavy tars by cooling the gas from 450 °C to just above the water dew point and secondly by absorption of light tars. The key philosophy in this is operating OLGA above the water dew point, while decreasing the tar dew point to a level under the lowest process temperature [28].

In the research centre BEST, a biodiesel scrubber is used, operated with Rapeseed methyl ester (RME). Syngas is cooled and injected into the scrubber at temperatures between 50–80 °C. Inside the scrubber, the tar from the syngas condenses and is absorbed by the RME at temperatures between 5–15 °C. For a 1 MW gasification pilot plant, approximately 60 l/h of biodiesel has to be replaced with new biodiesel. The high demand of biodiesel implies high variable costs. However, the regeneration of the biodiesel

can reduce the demand of biodiesel from 60 l/h to 5 l/h [75].

The most conventional way in the industry to separate tars is using cold gas cleaning methods. **Table 5** shows the tar removal efficiency for the most used cold gas cleaning methods.

Table 5: Particulate and tar removal efficiency for cold gas cleaning methods [27][85][86].

Methods	Particulate removal (%)	Tar removal (%)
Sand bed filter	70-99	50-97
Oil scrubber	n.a.*	64.5-96
Wash tower	60-98	10-25
Venturi scrubber	93-99.5	50-90
Wet electrostatic precipitator	>99	0-60
Fabric filter	70-95	0-50
Rotational particle separator	85-90	30-70
Fixed bed tar adsorber	n.a.*	50

*Data not available

Finally, an activated carbon guard can be implemented for further removal. This step is useful to protect further cleaning steps that requires the compression of the syngas, because, as said before, tar condensation in the compressor may lead to the malfunctioning of the equipment [4].

2.7.2 Sulfur removal and recovery

It is important for downstream applications to reduce the amount of acid gas from syngas. Using syngas for power generation requires to reduce the amount of H₂S to 10 ppmv, for chemical fuel production the value of H₂S has to be even lower, from 1 ppmv to less than 0.01 ppmv, depending on the choice of the synthesis process [19, 93-96]. As a consequence, physical and chemical absorption processes are usually the most common solutions.

Physical absorption methods are based on the acid gas solubility within the solvent. Acid gas solubility depends on the acid gas partial pressure and the system temperature. Higher acid gas partial pressures increase the acid gas solubility. Low temperatures increase acid gas solubility, but, in general,

temperature is not as critical as pressure [91]. Different organic solvents can be used to absorb acid gases, however, the most common solvents are methanol, which is used in the Rectisol process and a mixture of dimethyl ethers of polyethylene glycol, which is used in the Selexol process[11-12].

On the other hand, chemical solvents used for chemical absorption processes are based on a chemical reaction between the solvent and the acid gas [91]. One of the most common chemical solvents for acid gas cleaning is methyl diethanolamine (MDEA). MDEA reacts directly with H_2S to form an amine salt (methyldiethanolamine sulphide) [13].

To better understand the most suitable situations for each method, **Table 6** makes an overview of the different solutions to remove the sulfur content of the syngas. This table analyzes the removal efficiency, the typical operating temperature and pressure ranges and the exit gas quality.

Table 6: Comparison of conventional acid gas removal absorption methods [11][90].

Solvent	Mechanism	Removal efficiency (%)	Typical process conditions	Exit gas quality
MDEA	Chemical	H_2S : 98 - 99	T: 30 - 35 °C	H_2S : 10 - 20 ppmv
		CO_2 : ≤ 30	P: ≤ 2.94 MPa	
Selexol	Physical	H_2S : 99	T: 4 - 7 °C	H_2S : <30 ppmv
		CO_2 : variable	P: 6.87 MPa	
Rectisol	Physical	H_2S : 99.5 - 99.9	T: -70 - 60 °C	H_2S : < 0.1 ppmv
		CO_2 : 98.5	P: 8.04 MPa	CO_2 : down to few ppmv

When H_2S is absorbed by the solvent, the solvent needs to be regenerated in order to be used again. The desorbed sulfur can be recovered using Claus process. This process produces elemental sulfur as final product. The recovery of sulfur from the product gas avoids the emission of sulfur gases to the atmosphere and allows the use of the sulfur recovered for other purposes. Nevertheless, in the laboratory scale DFB gasification reactor analyzed in this work, the use of Selexol, Rectisol and specially Claus processes are not economically viable. Due to this, these processes should be considered only in industrial scale DFB gasification reactors [87].

2.7.3 Nitrogen removal

For the removal of nitrogen components from the product gas stream (mainly NH_3 and HCN), wet scrubbing is the most conventional mechanism. Wet scrubbers use water for NH_3 removal at low temperatures because it is a polar molecule and has high affinity with water. When a spray tower is used as a contacting device at ambient temperature, a removal efficiency of more than 99% can be achieved [14]. However, hot-gas clean-up systems are more energetically efficient, especially when a catalyst is used, because there is no need to reduce the syngas temperature to the ambient temperature [15].

Catalytic processes in hot-gas clean-up systems convert NH_3 to N_2 and H_2 with thermal catalytic decomposition. Ni-based catalysts have been proved to be the most efficient and can remove more than 88 % of the feed gas NH_3 [16]. The selection of the support plays a key role in the activity of supported nickel catalysts: stronger acidity tend to increase catalytic activity. The most common supports are ZrO_2 , MoO_3 and especially Al_2O_3 . Operational temperatures are between 800-900 °C to achieve a high level of ammonia removal and to avoid carbon deposition and degradation of the syngas [92]. While nickel based catalysts are very active in ammonia decomposition, their major drawback is catalyst deactivation mostly by the H_2S present on the syngas or due to CO coking [27]. The differences between these 2 removal methods are summarized in **Table 7**.

Table 7: Comparison between the most known alkaline gas removal methods [15][14][49].

Method	Removal efficiency (%)	Typical process conditions	Disadvantages	Advantages
Wet scrubber	NH_3 : 99	T: 20 °C P: 1 MPa	<ul style="list-style-type: none"> Syngas must be cooled and then heated for further applications 	<ul style="list-style-type: none"> Well developed and widely used
Thermal catalytic decomposition	NH_3 : ≥ 88	T: ≥ 600 °C P: ≥ 1 MPa	<ul style="list-style-type: none"> Catalyst poisoning Not widely used 	<ul style="list-style-type: none"> No heating or cooling are necessary

2.8 Fly char for gas cleaning

Biomass gasification is not competitive against fossil fuels yet. The valorisation of by-products is important in order to reduce the waste and costs. Char is one of these by-products and can be used in different ways depending on its carbon content. When the carbon content from char is high, one of the options is to upgrade it to activated carbon (AC). This application is very attractive for DFB process when using olivine as bed material. Bed material has an influence in char composition, in case of olivine, the content of heavy metals is higher. Consequently, it cannot be used in agriculture or for animal food [21].

Hot gas cleaning methods are being developed to mitigate wet scrubbers disadvantages. In some of them, AC can be used as a catalyst support to remove gasification impurities such as tars, H_2S , HCl , particulates, and alkali compounds. Nevertheless, AC is an expensive material. Due to this, the upgrading of the char from the gasification to AC has been researched. While gasification, the operational conditions in DFB process are similar to those applied on the production of AC, leading to the possibility of producing AC from upgrading the char from DFB gasification. The economic costs have been proved to be less than those from the commercial AC. AC must have BET surface areas in the range of 800 – 1300 m^2/g for these applications [20].

During gasification process in DFB process, steam can be used as a gasification agent. The char that results from the devolatilization of biomass mainly consists of carbon. During char gasification, steam removes carbon from the char matrix, a process that either widens the existing pores in the char or creates new ones. Nevertheless, to be able to use the AC from DFB gasification, $\geq 44\%$ of the char that results from the devolatilization of wood pellets must be converted by steam. This allows that the unconverted char to acquire a sufficient BET surface area ($> 800 \text{ m}^2/\text{g}$) to be used for gas cleaning. BET surface area depends on the char precursor and gasification conditions. When the right pore size cannot be achieved, a fluidized bed reactor for further activation is necessary [20].

Fly char obtained from the 100 kW TU Wien DFB gasifier has a very low BET surface respectively pore volume compared with commercial AC. This means that they are less efficient as commercial AC for adsorption purposes because they cannot adsorb as many volume of impurities. The low BET surface from char obtained from the gasification in the DFB process can be explained by the extremely low retention time of the fly char, leading to an incomplete upgrade of the AC. For this reason, an external upgrade should be required. **Table 8** shows a comparison between a commercial AC and the fly char obtained from the DFB gasification.

Table 8: Differences between fly char from DFB process and Commercial AC [20][59][78].

Fly char		Commercial AC
BET (cm²/g)	178.9	890.72
Pore size (nm)	4.08	2.13
Cost (€/kg)	0.23*	3.5
Elemental composition (% weight)	C	35.20%
	Al₂O₃	6.1%
	SiO₂	15.4%
	CaO	27.6%
	Na₂O	2.4%
	Fe₂O₃	2.6%
	K₂O	2.8%
	TiO₂	0.5%
	MgO	3.4%
	Others	4.1%

**The cost was calculated if the Fly char is externally upgraded to AC [20].*

The table above outlines the poor performance of fly char as an adsorbent. The very low BET surface area demonstrate that the commercial AC is more efficient and will have better results. The pore size of both samples is very similar, both are mesoporous materials but the pore size from fly char is slightly higher. The elemental composition is different, being the ash content in fly char is higher than the ash content of a commercial AC.

2.8.1 Synthesis of AC

To make DFB gasification process more competitive, a reduction of the operating costs of the cleaning process can be obtained by producing AC during the gasification process, thus reducing the quantity of commercial AC needed in the cleaning step.

The production of AC within the DFB reactor has been proved to be totally unattainable. Consequently, an external upgrade of the char produced inside the reactor has to be performed. There are 3 different mechanisms for the production of AC: physical activation, chemical activation and physiochemical activation [51].

Physical activation requires a high temperature between 800-1,100 °C in an oxidizing gas atmosphere such as steam, CO₂ or air. CO₂ is usually preferable as oxidizing gas. From an industrial perspective,

pure CO₂ is expensive and flue gas can be used instead for upgrading the char. However, the BET surface area will be lower (804 m²/g) than the BET surface area obtained from pure CO₂ (1,252 m²/g). The higher reactivity of steam activation results in high percentage of mesopores, whereas CO₂-activated carbon has up to 90% microporous structure [51].

Chemical activation is a single-stage (direct) process that includes an impregnation step prior to heat treatment in an inert atmosphere at temperature of 400–600 °C. Some chemicals that are widely used as activating agents are zinc chloride (ZnCl₂), potassium hydroxide (KOH), trihydroxidooxidophosphorus, phosphoric acid (H₃PO₄) and potassium carbonate (K₂CO₃) [51].

Lastly, AC can be produced by physiochemical activation. This process can be defined as an activation process involving the raw precursors/char impregnation, followed by heat treatment in presence of oxidising gas or by changing the atmosphere from N₂ to oxidising gas at an elevated temperature [51].

The most conventional way of heating the char for the activation is using an electric furnace. This system has a high energy consumption and low heat transfer efficiency. For these reasons, microwave heating systems are becoming more viable [52]. These systems have huge advantages with regard to electric furnaces, such as low operational costs or reduced processing time. Nevertheless, the capital investment in microwave systems is higher than in electric furnaces [50].

2.8.2 Gas cleaning processes

New ways to use the solid by-products of biomass gasification are being developed. One of them suggests the use of the solid by-products as catalysts for tar reforming. Tar reforming is a complex mechanism and it is not fully understood yet [22]. Normally, tar reforming is performed in a second reactor in series with the gasification reactor. The tar reforming reactor has a steel net to support the catalyst bed that is usually made of Ni supported by γ -Alumina or Ni-Co/Ce supported by γ -Alumina. The operation is performed at a temperature of 750 °C [57]. In the future, char could be used as a substitute of these expensive catalysts [22]. **Figure 20** shows a simplification of the complex reaction mechanism when char is used as catalyst for the tar reforming:

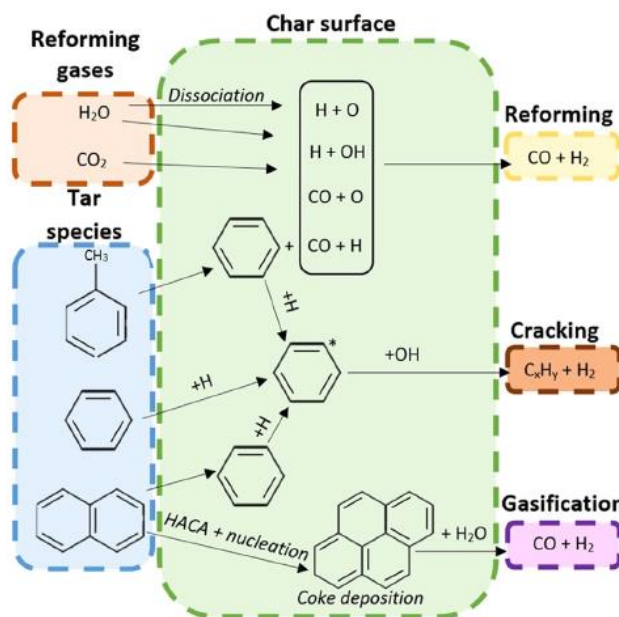


Figure 20: Simplified mechanism of the heterogeneous tar reforming reactions with a char based catalyst [22].

The use of regular char as catalyst for tar reforming has been studied resulting on almost 100 % conversion when the temperature is around 900 °C. Tar decomposition capabilities at this temperature are almost equal to those of Ni, which is the commercial catalyst for tar reforming. When using regular char, the distribution of the ashes over the char surface is important due to their elemental composition can lead to an improvement of the tar removal efficiency. The char can also be used as a supporter of different metals such as Fe, Ni, K and in a minor extent Ca and Co. The use of char as a support improves the process but makes it more expensive. Further research is needed in analyzing the activity of chars with different porous structures using different gasification agents at different temperatures. This can ultimately lead to a pure-char catalyst that provide a tar conversion efficiency as high as those obtained with Ni-based catalysts and lower economic costs [22].

Ashes play a key role in tar removal when using fly char as an adsorbent. **Table 8** shows that the ash content from fly char is very high with regard to commercial AC. CaO and other species present in ashes (Al_2O_3 , Fe_2O_3 , MgO and K_2O) adsorb CO_2 , shifting thermodynamic conditions to favour the decomposition of alkylbenzenes and the formation of H_2 , and may even prevent the formation of some tar species during gasification. Ni from the ashes could lead to more active sites on the catalyst surface for catalytic reforming reactions, thus leading to the higher tar conversion and the higher yield of H_2 [58].

Apart from tar reforming, other possible approach is the use of AC filters for tars and particles. Fe-supported activated carbon catalyst has been proved to reduce the amount of impurities. The results with two AC filters in series shows that the concentration of tar and particles might decrease from 2,428 to

102 mg/Nm⁻³ and from 2,244 to 181 mg/Nm⁻³, respectively [23].

2.8.3 Influence of ashes on char reactivity

During the gasification alkali and alkaline earth metallic (AAEM) species are produced due to the elemental composition of the fuel. AAEM can be separated in two groups, gas-phase AAEM species which are released along with the product gas and the solid-phase AAEM species, which impregnate the char and are considered as ashes. **Table 9** shows the elemental composition of sample of fly-char ashes obtained in a DFB gasification reactor. In this sample, the majority of the content from ashes are AAEM species, being the most relevant the Ca and the Si content that together forms the 66.37 % of the ashes content. Besides, the content of Mg, K and Na is important and although it is not as high as the content of Ca or Si, the sum of these 3 species forms the 13.22 % of the ashes content [60].

Table 9: Elemental analysis of a fly-char ashes sample obtained from DFB gasification.

Elemental composition of fly char ashes (wt%)_{db}												
CaO	SiO₂	Al₂O₃	MgO	K₂O	Fe₂O₃	Na₂O	SO₃	P₂O₅	MnO	TiO₂	ZnO	Others
42.58	23.79	9.37	5.27	4.3	4	3.65	2.29	1.86	0.78	0.71	0.43	0.97

The AAEM species have been proved to increase the reactivity of the char. The reactivity can be even higher if the volatile AAEM is absorbed in the char during the gasification and thus increasing the content of AAEM within the char. This can play a fundamental role because volatile AAEM have a higher influence in the catalytic activity from the char than solid AAEM. This can be caused by the more stable bonds between the volatile-phase AAEM and the char matrix or, due to a better dispersion of them in the char [60].

During the in-situ tar reforming, AAEM species on the surface of the char matrix act as active sites for tar reforming, affecting the evolution of the aromatic ring structure and oxygen-containing functional groups of the char-based catalyst and its pore structure. AAEM species active sites promote the increase of active intermediates (C-O bond and C-O-AAEMs), and enhances the interactions between char-based catalysts and biomass tar. The abundant AAEMs may lead to the conversion of O=C-O and C=O to C-O [61].

3 Experimental Setup of Fly char testing

Within the present project, the design of an external upgrade method for fly char to achieve a quality AC for tar cleaning purposes was executed. Therefore, the upgrade of the fly char was performed in a fixed bed reactor at 850 °C in several experiments with a different retention time. The generated product was finally analyzed using a surface area and porosity analyzer. It is aimed, that the resulting activated carbon should have a BET surface area similar to the commercial activated carbon.

3.1 Description of the test plant

The experimental procedure was executed on a test plant designed by TU Wien. The pilot plant shown in **Figure 21** consist of a cylindrical quartz reactor with an internal diameter of 3 mm (**Figure 22**) heated by an electrical heater.

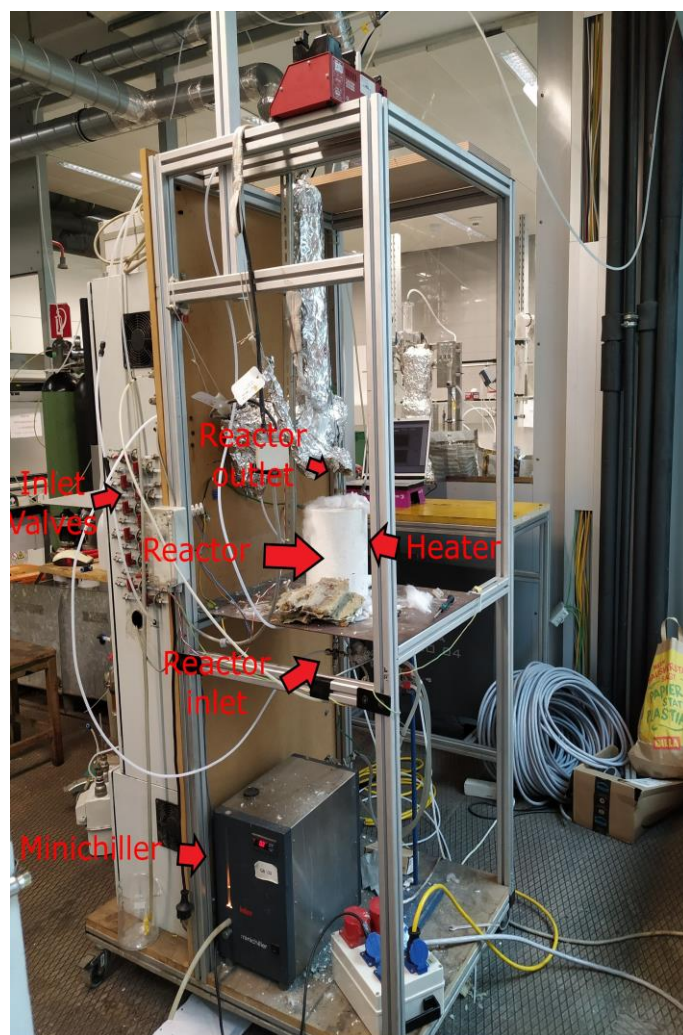


Figure 21: Pilot plant designed for the external physical activation of fly char.

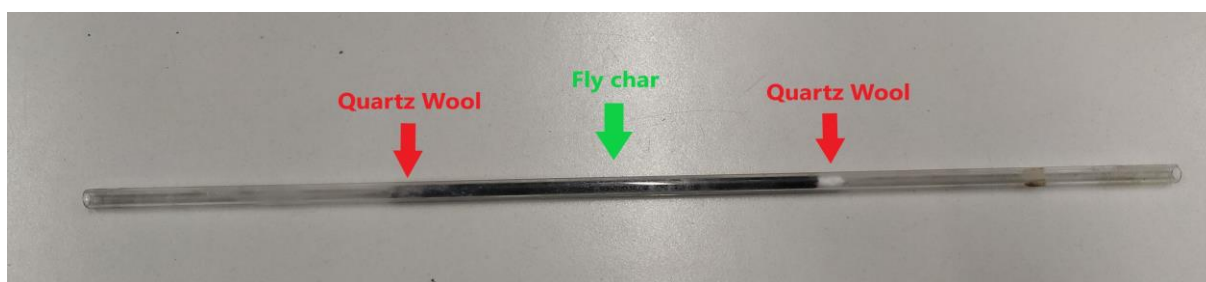


Figure 22: Reactor used for the experiments.

For the experiments, gas cylinders filled with nitrogen and carbon dioxide were used. Each cylinder was equipped with a pressure regulator to adjust 5 bar at the inlet of the mass flow controller. The gas supply was connected to the plant and the gas flowrate was accurately regulated by a valve connected to a mass flow controller prior to the reactor. After the electronic controller, a set of manual valves were used to close and open the flow of nitrogen and carbon dioxide. When the gas reached the reactor, it flowed through the quartz reactor from bottom to top making viable the option of a fluidized bed reactor. However, in these experiments the gas velocity was less than the minimum fluidization velocity, therefore, in practice, the model used was a fixed bed reactor. Moreover, the plant was equipped with three thermocouples and several gas flow meters to control the reactor temperature and the gas flowrate. Additionally, a continuous gas analyzer (**Figure 23**) was used to control the gas product composition and to confirm that the experiments are being realized successfully. Prior the continuous gas analyzer, a minichiller had to be deployed to cool the product gas due to the gas measurement device cannot withstand high temperature gases. This unit can be used not only for air cooling, but also for water cooling. For the experiment, it produced air at 0 °C. The gas product was cooled down with the cool air produced from the minichiller in a glass heat exchanger.



Figure 23: Continuous gas analyzer used during the experiments.

In the experiments, fly char (**Figure 24**) was activated using an external physical activation with CO_2 due to it has been concluded that it is not possible to produce activated carbon within the DFB gasification reactor because of the low retention time. The oxidizing agent and the carbon present on the sample reacted to produce CO according to **Eq. 11**, creating new pores and narrowing the existing ones in the sample.



The reason of using CO_2 instead of other oxidizing agents is that it is clean, easy to handle and facilitates the control of the process [62]. The fly char has been produced using wood as fuel in a DFB gasification reactor at the TU Wien.

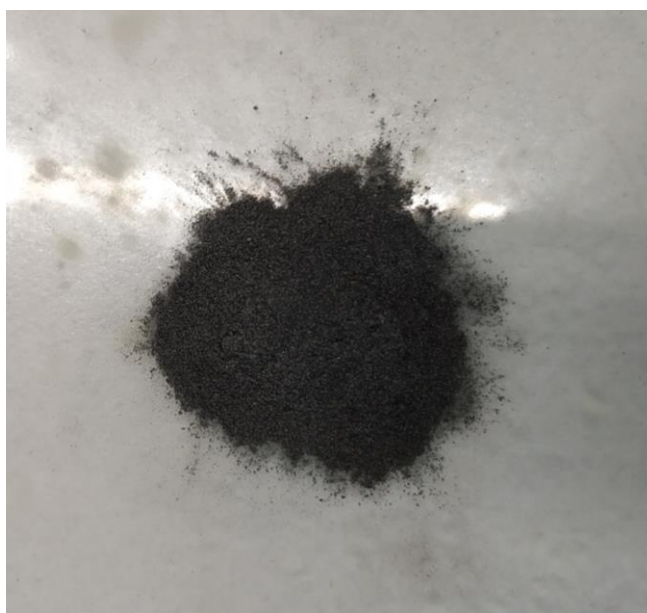


Figure 24: Fly char used as bed material.

The fly char used for the experiment had a pore size of 4.08 nm, which is higher than the pore size of a commercial AC (2-3 nm) and a BET surface area of 178.9 cm²/g, far below the BET surface area value for a commercial AC (>800 cm²/g) [20].

3.2 Experimental procedure

A previously dried sample of fly char obtained from the gasification reactor at TU Wien was introduced in the fixed bed reactor with quartz wool to prevent fly char leaks. The sample weight for each experiment was approximately 0.3 grams to avoid pressure drops due to the reactor length. The reactor was heated to 850 °C with an approximate heating rate of 11 °C/min via an electrical heating device while a flow of N₂ passed through the reactor. The choice of a heating rate value has been proved to have no effects on the final product [63]. For this reason, the heating rate chosen was the maximum heating rate that the electrical heater can reach. The N₂ flowrate chosen was 2 NI/h because of the pressure drop. The purpose of the nitrogen flow is to obtain an inert atmosphere in the reactor [20]. When the final temperature was reached, the nitrogen flow was switched to pure CO₂. Based on the literature, the recommended CO₂ flowrate range has been identified as 1.67 to 33.33 cm³/(min*g_{char}) [62]. Nevertheless, the CO₂ flowrate in the experiments was higher than the recommended flowrate due to the maximum recommended flowrate for a fly char sample of 0.3 grams (0.6 NI/h) is very low to be measured by the continuous gas analyzer.

For the experiments, different retention times were set because the surface area of the sample increases

with higher retention times. However, after a certain time, surface area decreases due to pore walls collapse [62]. An overview from the most important parameters for the experiments is showed in **Table 10**. As can be seen in this table, the chosen CO₂ flowrate was 1 NI/h for all the experiments with the exception of the first run. Taking into account the recommended CO₂ flowrate range, an average value of 0.45 NI/h was chosen for the first run, however, it was not possible to control the concentration of the outlet gas. The use of a flowrate value of 1 NI/h made the measurement of the outlet gas possible, but there was a delay on the concentration measurement due to the low CO₂ flowrate and the length of the tube between the outlet of the reactor and the continuous gas analyzer. In addition, the first two experiments were carried out twice because it was important to verify the correct operation of the plant during the first experiments and to repeat the first run with the same value of CO₂ flowrate as the other experiments. Moreover, as it will be further explained in **chapter 4.1**, it is not worthwhile with the selected parameters to conduct experiments with retention times higher than 2 hours.

Table 10: Parameters for the different experiments performed in the fixed bed reactor.

	m_{flychar} (g)_{db}	t (h)	Q_{CO₂} (NI/h)	Q_{N₂} (NI/h)	Temperature (°C)
Run 1	0.3755	0.5	0.45	2	850
Run 2	0.3324	1	1	2	850
Run 3	0.3601	2	1	2	850
Run 4	0.3419	1	1	2	850
Run 5	0.3656	0.5	1	2	850

While carrying out the experiments, the temperature from the inlet and outlet gas and the temperature inside the reactor were measured using thermocouples. The outlet gas must be cooled using air at 0 °C produced in an air cooler to be subsequently measured in a continuous gas analyzer. The presence of CO in the outlet gas indicates that the physical activation was being performed. When the previously stablished retention time was reached, the sample and the reactor were cooled using the same nitrogen flowrate as in the heating process. Finally, when the atmospheric temperature was reached, the product were removed from the reactor and replaced with another dried sample.

The product from the activation process must be subsequently analyzed in a surface area and porosity analyzer to determine if the final product can be considered as activated carbon.

4 Results

4.1 Results from experiments

The results obtained from the experiment showed a clear effect from the retention time as shown in **Table 11**. Generally, the mass loss confirms that the physical activation has been performed and the proper operation of the test plant. With the exception of the first run, it can be seen that when the retention time increases, there is a reduction of the activated carbon yield. This result is consistent because the CO_2 reacts with the carbon within the sample and produce CO , therefore, when the retention time is increased, less carbon remains in the product and the mass of the product decrease until there is no carbon to react. The activated carbon yield can be calculated from **Eq. 12**:

$$AC_{yield} = \frac{m_{AC}}{m_{fly\ char}} * 100 \quad (\text{Eq. 12})$$

To facilitate the comparison between each sample, a quality indicator for activated carbon (X_{AC}) has been defined in **Eq. 13**, the value resulted from this formula is related to the increase of surface area and the mass loss after the experiments. In this approach, a higher X_{AC} does not mean that the resulted sample has higher BET surface area, it could also be possible that an experiment with more activated carbon yield but with less BET surface had more X_{AC} than the process with a higher BET surface area product because of the difference in the final product mass.

$$X_{AC} = \frac{m_{AC} * BET_{AC}}{m_{fly\ char} * BET_{fly\ char}} \quad (\text{Eq. 13})$$

Table 11, overviews the results obtained from every experiment performed on the test plant and includes the calculations defined above to ease the comparison between the different outcomes. Unfortunately, it was not possible to perform the analysis with the surface area and porosity analyzer within the research period of the present work. Consequently, the results from the BET surface area and the pore size for each run are not included in **Table 11** and, therefore, the quality indicator cannot be calculated.

Table 11: Summary of the results obtained for each experiment.

	$m_{\text{fly char}}$ (g) _{db}	m_{AC} (g) _{db}	AC_{yield} (wt %) _{db}	t (h)	Q_{CO_2} (NI/h)
Run 1	0.3755	0.2723	72.52	0.5	0.45
Run 2	0.3324	0.2415	72.65	1	1
Run 3	0.3601	0.2481	68.90	2	1
Run 4	0.3419	0.2481	72.57	1	1
Run 5	0.3656	0.2834	77.52	0.5	1

The results obtained showed that increasing the retention time in the reactor, the AC_{yield} decreases. This means that the CO_2 is reacting with the carbon of the sample to create CO , thus creating new pores and narrowing the existing ones. Nevertheless, a surface area and porosity analysis is required to confirm that the pore size and the BET surface area have similar values to those of a commercial AC.

Visually, the results are not very clear and it is not possible to differentiate between products with higher surface area to others with less surface area. Nevertheless, when the carbon content is removed from the sample because of the reaction with CO_2 , the characteristic black color from carbon shifts to brown. It is important to remark that fly char composition is not only C, as it has been seen in **Table 8**, it has also a wide range of metals in its composition. The presence of these metals gives to the fly char a brown color when the carbon is exhausted. In run 3, the retention time was set to 2 hours, with the established carbon dioxide flowrate; the time was high enough to consume all the carbon from the sample. The consumption of the carbon is due to the reaction of carbon with CO_2 to produce CO . This phenomenon is shown in **Figure 25**.

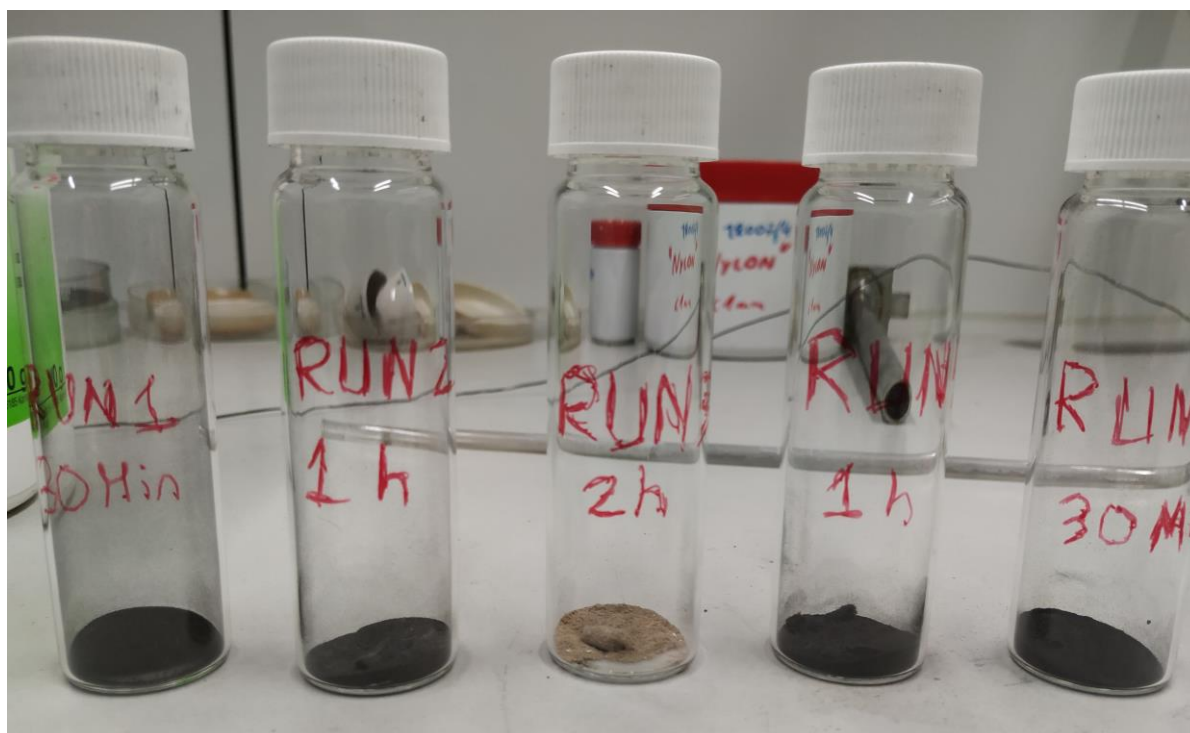


Figure 25: Product obtained from the different runs, ordered from left (Run 1) to right (Run 5).

The pore size has a key role in which tar compounds can be adsorbed and in the amount of adsorbed gas. The untreated fly char, which has a larger pore size than the commercial AC is less efficient for the adsorption of light and medium tar compounds due to its pore size. Nevertheless, it can be used for the adsorption of heavy tar compounds that cannot be adsorbed by the commercial AC. To have a better idea of which tar compounds can be adsorbed with a commercial AC, **Table 12** shows the critical diameter of a wide range of hydrocarbons (C_6 - C_{75}). The critical diameter has been obtained following the Van der Waals model. According to this table, the vast majority of the tar compounds produced in the gasification process can be adsorbed in a commercial AC, therefore, it is better to reduce the pore size from the fly char produced during gasification to increase the amount of adsorbed gas.

Table 12: Van der Waals diameter for selected tar compounds [64][65].

Molecular formula	Name	Critical diameter (nm)
C ₆ H ₆	Benzene	0.58
C ₇ H ₈	Toluene	0.63
C ₈ H ₁₈	Octane	0.73
C ₁₃ H ₂₈	Tridecane	0.88
C ₁₅ H ₃₂	Pentadecane	0.93
C ₂₀ H ₄₂	Eicosane	1.05
C ₂₅ H ₅₂	Pentacosane	1.14
C ₃₀ H ₆₂	triacontane	1.22
C ₃₈ H ₇₈	Octatriacontane	1.60
C ₄₃ H ₈₈	Tritetracontane	1.68
C ₅₀ H ₁₀₂	n-pentacontane	1.74
C ₆₀ H ₁₂₂	n-hexacontane	1.84
C ₇₀ H ₁₄₂	n-heptacontane	1.94
C ₇₅ H ₁₅₂	n-pentaheptacontane	2.00
C ₈₀ H ₁₆₂	n-octacontane	2.06

4.2 Proper choice for measurement device

Choosing a measurement device is not an easy task, there is not a universal solution for each component. Each measurement point has to be studied first in order to find a proper measurement technology. In this case, syngas is a complex mixture of different compounds and the objective is to be able to measure the main sulfur (H_2S and COS) and nitrogen (NH_3 and HCN) impurities up- and downstream the cleaning process. The design of the cleaning process is very important because particulate matter and condensed components can damage the measurement systems. As can be seen in **Figure 26**, a particle filter is used to eliminate particles like dust and char. After this step, the gas is led through six impinger bottles. The first two bottles are needed to condense water and heavy hydrocarbons that condense at temperatures higher than 4°C . The next three bottles are filled with RME, in this bottles tars are washed out of the gas. The last bottle ensures that no RME flows through the online gas measurement systems [82].

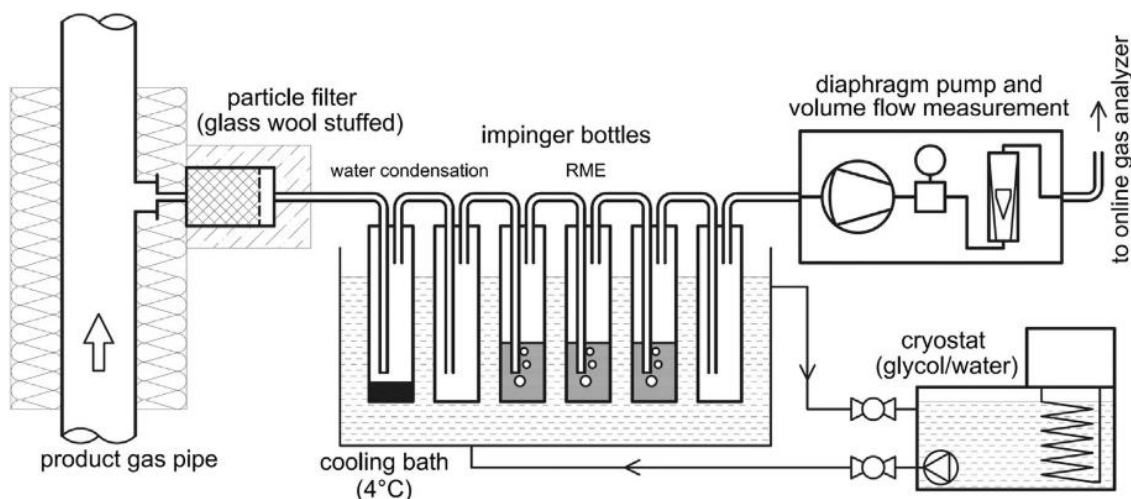


Figure 26: Current product gas cleaning process for online measurement [55].

It is important to keep in mind the other components of the gas mixture because in some devices they could affect the measurement, which is called cross-sensitivity. For instance, in FTIR, CO_2 overlaps with H_2S making H_2S difficult to measure [47].

To choose the measurement device, an approximate value of the components from the gas compound must be given. This can be obtained using an offline measurement technique such as wet chemical analysis. Wet chemical analysis includes two steps; the first one is the sampling of the target compounds capturing it with a solvent in impinger bottles. After sampling, an analysis of the resulting solution with different techniques must be done [47].

The chosen measurement devices should measure the gas product impurities up- and downstream the cleaning step. The concentration change must be considered because some devices are suitable

measuring high concentrations and others are more suitable for lower concentrations.

To test several measurement technologies, an experimental test-run in the 100 kW DFB from TU Wien was performed. In the test run, a GC-AED was used to measure sulfur impurities while a GC-MS was used to measure nitrogen impurities. Moreover, a FTIR was tested for nitrogen and sulfur impurities. These technologies were chosen because they were available in the university while other viable options such as GC-FPD or GC-PFPD for sulfur measurement or GC-NPD for nitrogen measurements were not available for testing. The measurements were taken up- and downstream the cleaning step. The measurements were taken at two points in time. At the first observation period softwood pellets were used as fuel in the 100 kW gasification plant and digestate pellets in the second.

4.2.1 Sulfur impurities measurement

GC technologies are the most common technologies for measuring sulfur compounds. In this case, H₂S and COS are the most interesting compounds due to their high concentration in the product gas. Over the years, gas chromatographers have become one of the most widely used methods of analytical chemistry [45]. The wide range of detectors developed makes GC very versatile and makes it suitable for measuring the raw and clean gas from the gasification process [29].

A GC equipped with a TCD is one of the most common detectors for high concentrations and has been proved to measure H₂S and COS with a detection limit of 10 ppmv in Energy research Centre of the Netherlands, part of The Netherlands Applied Research Organisation (ECN part of TNO) [37]. This is one of the most developed technologies and one of the cheapest [29]. Due to the low sensitivity of this detector, it can be used only before the cleaning process.

Sulfur-specific detector are much more sensitive than TCD. These detectors are the FPD, the PFPD and the SCD. FPD is the least sensitive of the 3 detectors and its range of measurement is from 0.02 ppmv to 120 ppmv. SCD is the most sensitive and can measure from 10 ppb for both sulfur impurities to up to 1,000 ppmv for H₂S compounds [37]. To choose the most suitable detector for low concentrations of sulfur, **Table 13** shows a comparison between these technologies.

Table 13: Comparison between different GC measurement technologies for low sulfur concentrations [37].

	TCD	FPD	PFPD	SCD
Ease of use	Easy	Easy	Moderate	Difficult
Price	€	€€	€€€	€€€€
Lower detection limits	10 ppmv	0,2 ppmv	50 ppbv	10 ppbv
Other elements detected	Universal	P, Sn	P	-
Cross-sensitivity	Water and tars	Hydrocarbon impurities	Hydrocarbon impurities	Benzene, thiophene, H ₂ S and H ₂
Advantages	<ul style="list-style-type: none"> • Very cheap • Minimal maintenance • Accurate measurement in complex gas mixtures 	<ul style="list-style-type: none"> • Cheap • Minimal maintenance 	<ul style="list-style-type: none"> • Linear response • Long-term calibration stability 	<ul style="list-style-type: none"> • No hydrocarbon quenching • Linear response
Disadvantages	<ul style="list-style-type: none"> • High lower detection limits 	<ul style="list-style-type: none"> • Non-linear response • Difficult calibration and quantification • Hydrocarbon quenching 	<ul style="list-style-type: none"> • Hydrocarbon quenching • The detector must be tuned for specific concentration ranges • Not compatible with packed columns 	<ul style="list-style-type: none"> • Complex maintenance • Reduction of response due to air leakage if proper vacuum is not maintained

Although FPD, PFPD and SCD can measure sulfur impurities in very low concentrations, they are not suitable to measure high concentrations of them, because of that, a TCD would be needed to measure high sulfur concentrations before the cleaning step. If the TCD is not available, a dilution of the sample gas can be applied in order to reduce the sulfur content of the sample. When measuring low concentrations of sulfur, an SCD cannot be recommended in this particular situation. Although it has some advantages such as the high sensitivity and the lack of hydrocarbon quenching, it is a costly technology that requires a skilful operator and has a complex maintenance compared to the other sulfur-specific detectors. Furthermore, the main sulfur compounds of the syngas can be measured using technologies with less sensitivity [37].

Finally, the other GC detectors considered in **chapter 2.5** are currently not advisable for this application. One of these detectors is the AED. AED is less sensitive than a PFPD, more expensive than the SCD and requires a regular maintenance. GC-MS is non-viable for this application because H_2S and COS peaks overlap with the peaks of other compounds due to the chemical complexity of the syngas. Furthermore, GC-MS is one of the most expensive detectors. A similar problem happens to BID. The chemical complexity of the syngas can saturate the detector, making peak separation challenging. Finally, the use of ELCD and PID have not been validated in gasifiers using different fuels, therefore, further research on these technologies has to be carried out in order to make them fully commercially available for gasifiers [37].

Due to the impossibility of using the recommended technologies, a GC-AED (**Figure 27**) was used to measure sulfur impurities in the experimental test-run. Two columns were used in series because COS and H_2S overlaps when using one column, these columns were an HP-5, which is a (5%-phenyl)-methylpolysiloxane nonpolar column and a RT-U-Bond, which is a divinylbenzene ethylene glycol/dimethylacrylate column.



Figure 27: GC-AED used for the sulfur impurities (H_2S , COS) measurement during the test-run.

The results obtained from the GC-AED are shown on **Table 14**. According to **chapter 2.4**, the sulfur impurities values when wood is used as fuel are much higher than the values obtained from previous measurements. Nevertheless, the value for the digestate pellets seems to fit with previous values. Another discordance is that the COS value is higher after the cleaning step according to the results from the GC-AED. To validate the results from the GC-AED during the operation with digestate pellets, the product gas before the cleaning step was also measured using the wet-chemical analysis. The results from the wet-chemical analysis showed a concentration of 1,008 ppmv for H_2S , which is a bit lower than the concentration measured with the GC-AED (1,221.3 ppmv). However, the concentration value obtained with GC-AED using wood as fuel was very high compared with the data gathered from other experiments. Further improvements, for example, in the calibration method can be undertaken to obtain more accurate results.

Table 14: Results from GC-AED for the different fuels used in the test-run.

		Wood	Digestate pellets
Before cleaning step	H_2S (ppmv)	511.1	1,221.3
	COS (ppmv)	6.5	15.0
After cleaning step	H_2S (ppmv)	461.7	841.7
	COS (ppmv)	8.4	36.2

Although this technology has been proved to work on other research centres for sulfur impurities measurement, it is not recommended as a solution for the test-plant in TU Wien because it has a relative

high cost and it has more difficult maintenance than other sulfur-selective detectors [37]. For this reason, if finally the gas chromatography technology is chosen for sulfur impurities measurement, the best options are the GC-FPD or the GC-PFPD.

Apart from GC technologies, other measurement technologies can be used for this application. For this reason, FTIR technology was tested not only for the nitrogen impurities measurements, as it will be deeply described in **chapter 4.2.2**, but also for sulfur impurities. According to bibliography, FTIR technology can be suitable for COS measurement but it is problematic to analyze H₂S when the sample has a high concentration of CO₂ in its composition. The results obtained during the test-run showed the inability to get neither COS measurements nor H₂S measurements. Nevertheless, this can be fixed with a future test improving the sampling or using a different setting of the FTIR. An alternative for FTIR could be the use of QCL. This technology can measure not only the main sulfur compounds, but also the main nitrogen compounds. Nevertheless, it is not yet a fully mature technology, it requires a skilled operator and it can measure compounds if they are above 0.1 ppmv. This can be problematic in the FT process, where the impurity content must be very low. Finally, the use of UV-VIS and NDIR are discarded for this application. Due to the complexity of the product gas, the use of an UV-VIS to quantify individual compounds of the product gas can be very challenging. However, it has been proved to be accurate when measuring the total amount of sulfur. With regard to NDIR, the sensitivity of this technology is very low for this application (200 ppmv) [37, 47].

4.2.2 Nitrogen impurities measurement

FTIR is the most preferred technology for nitrogen impurities online measurement among the IEA Bioenergy contributing partners [37]. The reasons are very clear, FTIR (**Figure 28**) can analyze a sample in the order of seconds, has high sensitivity, it is way cheaper and simpler than the GC solutions for these components (MSD, NCD, NPD). In addition, FTIR can measure water as well as other compounds (e.g. HCl) which are very problematic for TCD (TCD can only analyze a concentration of NH₃ higher than 500 ppm) and other GC technologies [47]. However, FTIR has also its downsides. According to the research centres that use this technology (BE2020+, CEA, DTU, TU Delft), when sampling, the gas must be diluted in a dilution system in order to prevent FTIR analysis chamber saturation of the gas matrix [37]. In addition, the sample gas must not be a tar-loaded gas. Finally, it seems that high concentrations of H₂O can induce an important error (close to 50%) on the NH₃ quantification by FTIR if H₂O is not taken into account in the calibration method. Therefore, in order to address this effect of collisional broadening, a mathematical model has to be used [47]. With regard to the gas chromatography technologies, it has been concluded at Iowa State University that the GC-NCD can be used to measure the product gas from gasification. This technology can detect nitrogen to ultra-low detection limits, being the lower detection limit 10 ppbv. The implementation of a GC-NPD could be

also possible but there is no evidence of the use of this technology for product gas from gasification [37]. Nevertheless, if there are no interesting phosphorous compounds to measure on the sample, it is a worse option than GC-NCD because of the higher maintenance costs and lower accuracy [81]. Due to that, this technology will not be considered for this application. Finally, as it has been discussed in **chapter 4.1.1**, QCL could be an interesting technology for this application.



Figure 28: Example of a FTIR measurement device [88].

During the test-run of the 100 kW DFB gasification reactor at TU Wien, a FTIR and a GC-MS (**Figure 29**) were used for the analysis of nitrogen impurities. The implementation of a GC-NCD was suggested but this technology was not available.



Figure 29: GC-MS used for the nitrogen impurities (NH_3 , HCN) measurement during the test-run.

For the analysis using GC-MS, the column used analysis was a RT-U-BOND (divinylbenzene ethylene glycol/dimethylacrylate). The results obtained from this technology did not match with any previous results, therefore, they were discarded. Although GC-MS could work for syngas measurement, it is not recommended for this application because NCD is much cheaper and the operation is simpler [65].

5 Conclusion and outlook

The present work was developed with the aim of finding answers to the research question "what sulfur and nitrogen gas measurement technologies are the most reliable, cheap, fast and easy to handle for a DFB gasification reactor?" and to the research question "Is it possible to perform an external upgrade for the fly char produced in the DFB gasification reactor?".

A bibliographical research was conducted to evaluate the state of art of the DFB gasification reactor, different synthesis methods, product gas composition from different fuels used in gasification, online gas measurement technologies, especially for nitrogen and sulfur impurities, fly char properties and gas cleaning technologies emphasizing the use of fly char and activated carbon for tar cleaning.

With regard to gas measurement technologies, the outcome from the bibliographical research was that gas chromatography, infrared spectroscopy and adsorption spectroscopy, were the most used technologies for analyzing gasification processes. The choice of a proper detector and column for each application in gas chromatography is crucial. Each detector has its advantages and disadvantages, and therefore, there is no detector that can be easily adapted to every situation. Thus, the most recommended sulfur detectors are TCD for high concentrations and FPD or PFPD for low concentrations. In the case of nitrogen measurement, the preferred choice is the NCD. Although gas chromatographers are the preferred choice to measure sulfur impurities there are other technologies available. Concerning adsorption spectroscopy, TDLAS coupled with a QCL can be calibrated to measure the main nitrogen and sulfur compounds, however, the calibration has been proved very challenging and is not a mature technology yet. Apart from GC detectors and adsorption spectroscopy, infrared spectroscopy is widely used for nitrogen impurities measurements in gasifiers and it could be possible to measure the main sulfur compounds from the gasifier.

To test several measurement technologies, an experimental test-run of the 100 kW DFB gasification plant was conducted at TU Wien. For the experiments, two different fuels were used, softwood and digestate pellets. The product gas from the gasification of both fuels was analyzed before and after the cleaning step and compared with other previous measurements to validate it. The measurement of H_2S and COS was performed offline in a GC-AED, while the measurement of NH_3 and HCN was performed offline in a GC-MS. The four compounds were also measured online in a FTIR. Although all of these technologies are supposed to be able to accurately measure the compounds selected, the outcome from the experiments did not fit with previous wet chemical measurements. This could be caused by the calibration method, the setup or the sampling. Although they could work on a future attempt, the use of GC-MS and GC-AED is not recommended for this application because of the high price of these technologies and their challenging implementation [37].

Table 15 and **Table 16** summarize the bibliographical research for the most recommended technologies, thus facilitating the comparison between these technologies and the correct choice for future

applications. In these tables, technologies are evaluated depending on their technology readiness level (TRL), operational expenditures (OPEX), capital expenditures (CAPEX), handling, measurement range and cross-sensitivity. Mature and widely used technologies are more recommended than recent technologies. Low OPEX and CAPEX are also preferable. An easy technology will be preferred and the measurement range will have to be considered in the upgrade process of the syngas. Finally, cross-sensitivity has to be evaluated due to the cleaning step will have to be adapted to the measurement technology chosen.

Table 15: General comparison between different selected sulfur measurement technologies [37][44][45][47].

	<i>TRL</i>	<i>OPEX/CAPEX</i>	<i>Handling</i>	<i>Measurement range</i>	<i>Cross-sensitivity</i>
<i>FTIR</i>	++	+/+	+	>0.3 ppmv	Tar-loaded gas. H ₂ , H ₂ O, CO ₂
<i>QCL</i>	-	-/-	--	> 0.1 ppmv	Particulate matter
<i>GC-TCD</i>	++	++/++	++	> 10 ppmv	Water and tars
<i>GC-FPD</i>	++	+/+	+	0.2 - 120 ppmv	Hydrocarbon impurities
<i>GC-PFPD</i>	++	-/-	-	> 50 ppbv	Hydrocarbon impurities

Table 16: General comparison between different selected nitrogen measurement technologies [37][44][45][47][69].

	<i>TRL</i>	<i>OPEX/CAPEX</i>	<i>Handling</i>	<i>Measurement range</i>	<i>Cross-sensitivity</i>
FTIR	++	+/+	+	> 0.3 ppmv	Tar-loaded gas H ₂ , H ₂ O, CO ₂
QCL	-	-/-	--	> 0.1 ppmv	Particulate matter
GC-NCD	+	--/--	-	> 10 ppbv	CO ₂ , CO, H ₂ O, O ₂ , H ₂ , Ar
GC-TCD	++	++/++	++	> 10 ppmv*	Water and tars

*For NH₃, the lower limit of detection is 500 ppmv

With regard to the physical activation, a bibliographical research was conducted in order to find the correct operational parameters of the process. The physical activation of a sample of dried fly char obtained from a DFB gasification reactor using wood as fuel was conducted with different retention times in a test-plant in TU Wien. With the selected operational parameters and with a retention time of 2 hours, the sample changed its color from black to brown. The reason of this phenomenon was the exhaustion of the carbon present in the sample. On the other hand, according to the critical diameter obtained from the Van der Waals model, the use of the untreated fly char is not recommended for tar adsorption purposes due its large pore size. Decreasing the pore size from the untreated fly char is crucial to increase the adsorption efficiency. For a commercial AC with a pore size 2 nm, it has been concluded that it can adsorb C₆-C₇₅ tar compounds, which is the vast majority of the tar compounds generated from the gasification process. A treated fly char with a pore size less than 2 nm would be more efficient than the commercial AC in the adsorption of light hydrocarbons but it could not adsorb heavy hydrocarbons. Nevertheless, if the pore size were bigger than the commercial AC, the treated fly char would be less efficient for tar cleaning purposes. Finally, the results obtained from the upgraded fly char showed that when the retention time increases, the resulting mass from the upgraded fly char decreases. This means that carbon is reacting with CO₂ to generate CO, thus decreasing the amount of carbon in the fly char. This was visually confirmed when a retention time of 2 hours was set and the fly char turned from black to brown.

Further research should be done:

- Evaluating the mistakes done when using the FTIR for online analysis, especially for nitrogen measurements.
- Considering the use of a gas chromatographer if the FTIR do not show good results on sulfur measurements in future test-runs.
- Reviewing the gas measurement technologies focusing on tar measurement.
- Increasing the size of the reactor for future fly char physical activation to use the recommended flowrate and to avoid big pressure drops and measurement delays.
- Optimizing the process carrying out experiments with multiple retention times to improve the quality of the product.
- Analyzing the upgraded fly char in a surface area and porosity analyzer.

6 Notation

Symbols

H ₂ O	Water	mol
CH ₄	Methane	mol
C _x H _y	Hydrocarbon	mol
H ₂	Hydrogen	mol
N ₂	Nitrogen	mol
O ₂	Oxygen	mol
O ₃	Ozone	mol
CO	Carbon monoxide	mol
CO ₂	Carbon dioxide	mol
H ₂ S	Hydrogen sulfide	mol
COS	Carbonyl sulfide	mol
NH ₃	Ammonia	mol
HCN	Hydrogen cyanide	mol
ZnCl ₂	Zinc chloride	mol
KOH	Potassium hydroxide	mol
H ₃ PO ₄	Phosphoric acid	mol
K ₂ CO ₃	Potassium carbonate	mol
CaO	Calcium oxide	mol
CaCO ₃	Calcium carbonate	mol
SiO ₂	Silicon dioxide	mol
Al ₂ O ₃	Aluminium oxide	mol
MgO	Magnesium oxide	mol
K ₂ O	Potassium oxide	mol
Fe ₂ O ₃	Ferric oxide	mol

Na ₂ O	Sodium oxide	mol
SO ₃	Sulfur trioxide	mol
P ₂ O ₅	Phosphorus pentoxide	mol
MnO	Manganese (II) oxide	mol
TiO ₂	Titanium dioxide	mol
ZnO	Zinc oxide	mol
X _{AC}	Quality indicator for AC	-
AC _{yield}	Activated carbon yield	wt % _{db}
Q _x	Volume flow of gas	Nl/h

Abbreviations

DFB	Dual fluidized bed
GR	Gasification reactor
CR	Combustion reactor
SER	Sorption enhanced reforming
WGS	Water-gas shift
GHG	Greenhouse gases
OPEX	Operational Expenditures
CAPEX	Capital Expenditures
TRL	Technology Readiness Level
AAEM	Alkali and alkaline earth metallic
AC	Activated carbon
BET	Brunauer-Emmett-Teller
FT	Fischer-Tropsch
GC	Gas chromatography

NCD	Nitrogen chemiluminiscence detector
NPD	Nitrogen-phosphorus detector
MSD	Mass spectroscopy detector
TCD	Thermal conductivity detector
SCD	Sulfur chemiluminiscence detector
FPD	Flame photometric detector
PFPD	Pulsed flame photometric detector
PID	Photoionization detector
ELCD	Electrolytic capture detector
AED	Atomic emission detector
BID	Barrier ionization detector
TDLAS	Tunable diode laser adsorption spectroscopy
QCL	Quantum cascade laser
FTIR	Fourier-transformed infrared spectroscopy
UV-VIS	Ultraviolet Visible
NDIR	Non-Dispersive Infrared
CON-TAR	Continuous tar analyzer
OLGA	Oil-based gas washing process
MDEA	Methyl diethanolamine
DME	Dimethylether
SNG	Synthetic natural gas
VOC	Volatile organic compounds
IEA	International energy agency
ECN	Energy Research Centre Netherlands
TNO	Netherlands organisation for applied scientific research
CEN	European committee for standarization

TS	Technical specification
RME	Rapeseed methyl ester
ECN	Energy Research Centre Netherlands
EU	European Union
U.S.	United States
ppmv	Parts per million volume
ppbv	Parts per billion volume
NI	Gas litre according to standard conditions (0 °C, 1.013 bar _{abs})
wt-%	Percentage by weight
wt-% _{db}	Percentage by weight on dry basis

7 List of tables

Table 1: Average values for the impurities and the main gas components in the product gas generated during gasification before the cleaning step [4, 10].	11
Table 2: Range of the impurity contents in the product gas and overview of the N- and S- impurity limits for different synthesis processes [4, 10, 19, 93-96].	12
Table 3: Approximate response of compound classes by PID [39].	20
Table 4: Comparison between cold, warm and hot gas cleaning technologies [14].	33
Table 5: Particulate and tar removal efficiency for cold gas cleaning methods [27][85][86].	35
Table 6: Comparison of conventional acid gas removal absorption methods [11][90].	36
Table 7: Comparison between the most known alkaline gas removal methods [15][14][49].	37
Table 8: Differences between fly char from DFB process and Commercial AC [20][59][78].	39
Table 9: Elemental analysis of a fly-char ashes sample obtained from DFB gasification.	42
Table 10: Parameters for the different experiments performed in the fixed bed reactor.	47
Table 11: Summary of the results obtained for each experiment.	49
Table 12: Van der Waals diameter for selected tar compounds [64][65].	51
Table 13: Comparison between different GC measurement technologies for low sulfur concentrations [37].	54
Table 14: Results from GC-AED for the different fuels used in the test-run.	56
Table 15: General comparison between different selected sulfur measurement technologies [37][44][45][47].	61
Table 16: General comparison between different selected nitrogen measurement technologies [37][44][45][47][69].	62

8 List of figures

Figure 1: Global anthropogenic CO₂ emissions from the most CO₂-intensive human activities [1].	1
Figure 2: Future industrial applications of biomass gasification technology [4].	4
Figure 3: Schematic diagram of the DFB gasification reactor from TU Wien [17].	6
Figure 4: Different ways for syngas utilization [5].	7
Figure 5: Path to different products via FT-synthesis [8].	9
Figure 6: Example of a gas sampling valve [66].	13
Figure 7: Most suitable stationary phases for every polarity case [58].	14
Figure 8: Block diagram of a chromatographic system [67].	15
Figure 9: Schematic of a typical TCD Wheatstone Bridge [29].	16
Figure 10: Flame Photometric Detector [40].	17
Figure 11: Detection process of a PFPD [29].	18
Figure 12: Block diagram of a CLD [29].	19
Figure 13: Schematic of an ELCD [29].	21
Figure 14: Detailed look at AED detection processes [29].	22
Figure 15: Compounds measured by the QCL system. [44]	24
Figure 16: Simplified layout of an FTIR spectrometer [47].	25
Figure 17: Schematic of a NDIR Analyzer Module [89].	26
Figure 18: Schematics of the tar sampling method in the pilot plant from TU Wien [55].	30
Figure 19: General diagram of a FID [47].	31
Figure 20: Simplified mechanism of the heterogeneous tar reforming reactions with a char based catalyst [22].	41
Figure 21: Pilot plant designed for the external physical activation of fly char.	43
Figure 22: Reactor used for the experiments.	44
Figure 23: Continuous gas analyzer used during the experiments.	45
Figure 24: Fly char used as bed material.	46

Figure 25: Product obtained from the different runs, ordered from left (Run 1) to right (Run 5).	50
Figure 26: Current product gas cleaning process for online measurement [55].	52
Figure 27: GC-AED used for the sulfur impurities (H₂S, COS) measurement during the test-run.	56
Figure 28: Example of a FTIR measurement device [88].	58
Figure 29: GC-MS used for the nitrogen impurities (NH₃, HCN) measurement during the test-run.	58

9 References

- [1] Intergovernmental panel on climate change (2014): Climate Change 2014: Synthesis Report. Retrieved from:
https://www.ipcc.ch/site/assets/uploads/2018/05/SYR_AR5_FINAL_full_wcover.pdf
- [2] United Nations Framework Convention on Climate Change (2015). Adoption of the Paris Agreement. Retrieved from: <https://undocs.org/FCCC/CP/2015/L.9/Rev.1>
- [3] European Commission (2020). Progress made in cutting emissions. Retrieved from:
https://ec.europa.eu/clima/policies/strategies/progress_en
- [4] Schmid, J. C., Benedikt, F., Fuchs, J., Mauerhofer, A. M., Müller, S., & Hofbauer, H. (2019). Syngas for biorefineries from thermochemical gasification of lignocellulosic fuels and residues - 5 years experience with an advanced dual fluidized bed gasifier design. *Biomass Conversion and Biorefinery*. <https://doi.org/10.1007/s13399-019-00486-2>
- [5] Hofbauer, H. (2013). Biomass Gasification for Electricity and Fuel, Large Scale. *Renewable Energy Systems*, 1422–1452. <https://doi.org/10.1007/978-1-4614-5820-3>
- [6] Schildhauer, T. J., & Biollaz, S. M. A. (2016). Synthetic Natural Gas from Coal and Dry Biomass, and Power to Gas Applications. John Wiley & Sons, Inc.
<https://doi.org/10.1002/9781119191339>
- [7] France, L. J., Edwards, P. P., Kuznetsov, V. L., & Almegren, H. (2015). The Indirect and Direct Conversion of CO₂ into Higher Carbon Fuels. *Carbon Dioxide Utilisation*, 161–182. <https://doi.org/10.1016/B978-0-444-62746-9.00010-4>
- [8] Speight, J. G. (2016). Introduction to fuel flexible energy. *Fuel Flexible Energy Generation*, 3–27. <https://doi.org/10.1016/B978-1-78242-378-2.00001-8>
- [9] Wilk, V. (2013). Extending the range of feedstock of the dual fluidized bed gasification process towards residues and waste. PhD Thesis. Vienna University of Technology.
- [10] Veress, M. (2016). Brennstoffkennwerte für die Biomassevergasung. Bachelor thesis. Vienna University of Technology.
- [11] Abdoulmoumine, N., Adhikari, S., Kulkarni, A., & Chattanathan, S. (2015). A review on biomass gasification syngas cleanup. *Applied Energy*, 155, 294–307.
<https://doi.org/10.1016/j.apenergy.2015.05.095>
- [12] Mondal, P., Dang, G. S., & Garg, M. O. (2011). Syngas production through gasification and cleanup for downstream applications - Recent developments. *Fuel Processing Technology*, 92(8), 1395–1410. <https://doi.org/10.1016/j.fuproc.2011.03.021>
- [13] Pal, P., Abukashabeh, A., Al-Asheh, S., & Banat, F. (2015). Role of aqueous methyldiethanolamine (MDEA) as solvent in natural gas sweetening unit and process contaminants with probable reaction pathway. *Journal of Natural Gas Science and Engineering*, 24, 124–131. <https://doi.org/10.1016/j.jngse.2015.03.007>

- [14] Malicha, M. (2018). Design of gas cleaning processes for SNG- production from biogenic residues. Bachelor thesis. Vienna University of Technology.
- [15] Zhang, W., Liu, H., Ul Hai, I., Neubauer, Y., Schröder, P., Oldenburg, H., Kolling, A. (2012). Gas cleaning strategies for biomass gasification product gas. *International Journal of Low-Carbon Technologies*, 7(2), 69–74. <https://doi.org/10.1093/ijlct/ctr046>
- [16] Dou, B., Zhang, M., Gao, J., Shen, W., & Sha, X. (2002). High-temperature removal of NH₃, organic sulfur, HCl, and tar component from coal-derived gas. *Industrial and Engineering Chemistry Research*, 41(17), 4195–4200. <https://doi.org/10.1021/ie010913h>
- [17] Schmid, J.(2014). Development of a Novel Dual Fluidized Bed Gasification System. Bachelor thesis. Vienna University of Technology.
- [18] European Commission (2020). What is the share of renewable energy in the EU? Retrieved from: <https://ec.europa.eu/eurostat/cache/infographs/energy/bloc-4c.html>
- [19] Molino A., Larocca V., Chianese S. et al. (2018). Biofuels Production by Biomass Gasification: A Review. *Energies*, 11, 4, 811. <https://doi.org/10.3390/en11040811>
- [20] Tchoffor, P. A., Davidsson, K. O., & Thunman, H. (2015). Production of activated carbon within the dual fluidized bed gasification process. *Industrial and Engineering Chemistry Research*, 54(15), 3761–3766. <https://doi.org/10.1021/ie504291c>
- [21] IEA Bioenergy Task 33 (2018). Valorization of By- Products from Small Scale Thermal Gasification. Retrieved from: <http://www.ieatask33.org/app/webroot/files/file/publications/Byproducts/Valorisation-of-byproducts.pdf>
- [22] Buentello-Montoya, D. A., Zhang, X., & Li, J. (2019). The use of gasification solid products as catalysts for tar reforming. *Renewable and Sustainable Energy Reviews*, 107, 399–412. <https://doi.org/10.1016/j.rser.2019.03.021>
- [23] Hanaoka, T., Matsunaga, K., Miyazawa, T., Hirata, S., & Sakanishi, K. (2012). Hot and dry cleaning of biomass-gasified gas using activated carbons with simultaneous removal of tar, particles, and sulfur compounds. *Catalysts*, 2(2), 281–298. <https://doi.org/10.3390/catal2020281>
- [24] Rönsch, S., Schneider, J., Matthischke, S., Schlüter, M., Götz, M., Lefebvre, J., Bajohr, S. (2016). Review on methanation - From fundamentals to current projects. *Fuel*, 166, 276–296. <https://doi.org/10.1016/j.fuel.2015.10.111>
- [25] Davis, B. H. (2005). Fischer-Tropsch synthesis: Overview of reactor development and future potentialities. *Topics in Catalysis*, 32(3–4), 143–168. <https://doi.org/10.1007/s11244-005-2886-5>
- [26] Devi, L., Ptasiński, K. J., & Janssen, F. J. J. G. (2003). A review of the primary measures for tar elimination in biomass gasification processes. *Biomass and Bioenergy*, 24(2), 125–140. [https://doi.org/10.1016/S0961-9534\(02\)00102-2](https://doi.org/10.1016/S0961-9534(02)00102-2)

- [27] Prabhansu, M. K., Chandra, P., & Chatterjee, P. K. (2015). A review on the fuel gas cleaning technologies in gasification process. *Journal of Environmental Chemical Engineering*, 3(2), 689–702. <https://doi.org/10.1016/j.jece.2015.02.011>
- [28] Zwart, R. W. R., Van Der Drift, A., Bos, A., Visser, H. J. M., Cieplik, M. K., & Könemann, H. W. J. (2009). Oil-Based gas washing- flexible tar removal for high-efficient production of clean heat and power as well as sustainable fuels and Chemicals. *Environmental Progress and Sustainable Energy*, 28(3), 324–335. <https://doi.org/10.1002/ep.10383>
- [29] Klee, M. S. (2012). Detectors. *Gas Chromatography*, 307–347. <https://doi.org/10.1016/B978-0-12-385540-4.00012-2>
- [30] Li, D., Liu, S., Li, D., & Liu, S. (2019). Drinking Water Detection. *Water Quality Monitoring and Management*, 251–267. <https://doi.org/10.1016/B978-0-12-811330-1.00010-7>
- [31] Rockwood, A. L., Kushnir, M. M., & Clarke, N. J. (2018). Mass Spectrometry. *Principles and Applications of Clinical Mass Spectrometry Small Molecules, Peptides, and Pathogens*, 33-65. <https://doi.org/10.1016/B978-0-12-816063-3.00002-5>
- [32] Yan, X. (2006). Unique selective detectors for gas chromatography: Nitrogen and sulfur chemiluminescence detectors. *Journal of Separation Science*, 29(12), 1931–1945. <https://doi.org/10.1002/jssc.200500507>
- [33] Doyle, W. M. (1992). Principles and applications of fourier transform infrared (FTIR) process analysis. *Process Control and Quality*, 2(1), 11–41.
- [34] Chasteen, T.G. Atomic Emission Detector. Sam Houston State University. Retrieved from: https://www.shsu.edu/~chm_tgc/primers/pdf/AED.pdf
- [35] Ingenieria Analytica (1992). Introducing an Improved Electrolytic Conductivity Detector for Gas Chromatographic Analysis of Pesticides. Retrieved from: http://www.ingenieria-analitica.com/downloads/dl/file/id/1025/product/90/the_introduction_of_an_improved_elcd_for_gas_chromatographic_analysis_of_pesticides.pdf
- [36] Byrd, G. D. (1999). Use of gas chromatographic and mass spectrometric techniques for the determination of nicotine and its metabolites. *Analytical Determination of Nicotine and Related Compounds and Their Metabolites*, 191–224. <https://doi.org/10.1016/B978-044450095-3/50007-3>
- [37] IEA Bioenergy Task 33. (2018). Gas analysis in gasification of biomass and waste - Guideline report - Document 1. Retrieved from: [http://www.ieatask33.org/app/webroot/files/file/publications/Gas analysis report/IEA Bioenergy Task 33 gas analysis report - Document 1.pdf](http://www.ieatask33.org/app/webroot/files/file/publications/Gas_analysis_report/IEA_Bioenergy_Task_33_gas_analysis_report_-_Document_1.pdf)
- [38] Medhe, S. (2018). Chemical and Biomolecular Engineering Mass Spectrometry: Detectors Review. *Mass Spectrometry: Detectors Review Article in Annual Review of Chemical and Biomolecular Engineering*, 3(4), 51–58. <https://doi.org/10.11648/j.cbe.20180304.11>

- [39] RAE Systems Inc. (2013). The PID Handbook. Retrieved from:
https://www.raesystems.com/sites/default/files/content/resources/pid_handbook_1002-02.pdf
- [40] Emerson (2014). FPD for Gas Chromatographs Hardware Reference Manual. Retrieved from: <https://www.emerson.com/documents/automation/manual-flame-photometric-detector-for-gc-hardware-reference-manual-rev-b-rosemount-en-72510.pdf>
- [41] Chambers, L., & Duffy, M. L. (2003). Determination of Total and Speciated Sulfur Content in Petrochemical Samples Using a Pulsed Flame Photometric Detector. *Journal of Chromatographic Science*, 41(10), 528–534.
<https://doi.org/10.1093/chromsci/41.10.528>
- [42] Shimadzu (2014). New Applications Using GC BID Detector. Retrieved from:
<https://solutions.shimadzu.co.jp/an/n/en/gc/sic114141.pdf>
- [43] Wall, K. J. (2006). A Review of Tunable Diode Laser Absorption Spectroscopy (TDLAS). <https://www.doi.org/10.13140/RG.2.2.19384.65280>
- [44] Emerson. Multi-Component Gas Analysis with Expand Insight and Optimize Performance. Retrieved from:
<https://www.emerson.com/documents/automation/article-emerson-introduces-world%E2%80%99s-first-hybrid-qcl-tdl-multi-component-continuous-gas-analyzers-rosemount-en-us-94126.pdf>
- [45] Smolková-Keulemansová, E., & Feltl, L.. (1991). Chapter 10 - Gas chromatography. *Analysis of Substances in the Gaseous Phase*, 28, 223–462.
[https://doi.org/10.1016/S0166-526X\(05\)80100-X](https://doi.org/10.1016/S0166-526X(05)80100-X)
- [46] Petit, S., & Madejova, J. (2013). Fourier Transform Infrared Spectroscopy. *Developments in Clay Science*, 5, 213–231. <https://doi.org/10.1016/B978-0-08-098259-5.00009-3>
- [47] IEA Bioenergy Task 33. (2018). Gas analysis in gasification of biomass and waste - Guideline report - Document 2. Retrieved from: https://www.ieabioenergy.com/wp-content/uploads/2018/09/Gas_analysis_report_II-1.pdf
- [48] LibreTexts. *How and FTIR spectrometer operates*. Retrieved from:
https://chem.libretexts.org/Core/Physical_and_Theoretical_Chemistry/Spectroscopy/Vibrational_Spectroscopy/Infrared_Spectroscopy/How_an_FTIR_Spectrometer_Operates
- [49] Wang, W., Padban, N., Ye, Z., Andersson, A., & Bjerle, I. (1999). Kinetics of ammonia decomposition in hot gas cleaning. *Industrial and Engineering Chemistry Research*, 38(11), 4175–4182. <https://doi.org/10.1021/ie990337d>
- [50] Rashidi, N. A., & Yusup, S. (2017). A review on recent technological advancement in the activated carbon production from oil palm wastes. *Chemical Engineering Journal*, 314, 277–290. <https://doi.org/10.1016/j.cej.2016.11.059>
- [51] Tadda, M.A., Ahsan, A., Shitu, A., ElSergany, M., Arunkumar, T., Jose, B., Razzaque, M., Abdur Daud, N.N., Nik (2016). A review on activated carbon: process, application

and prospects. *Journal of Advanced Civil Engineering Practice and Research*, 2(1), 7–13. <https://doi.org/10.1016/B978-1-59-749641-4.00015-1>

- [52] Yek, P. N. Y., Liew, R. K., Osman, M. S., Lee, C. L., Chuah, J. H., Park, Y. K., & Lam, S. S. (2019). Microwave steam activation, an innovative pyrolysis approach to convert waste palm shell into highly microporous activated carbon. *Journal of Environmental Management*, 236, 245–253. <https://doi.org/10.1016/j.jenvman.2019.01.010>
- [53] Chartered Institution of Wastes Management. Gasification. Retrieved from: <https://www.ciwim.co.uk/ciwim/knowledge/gasification.aspx>
- [54] Sam, A. (2019). Toxic Waste From Municipality. *Energy from Toxic Organic Waste for Heat and Power Generation*, 7–16. <https://doi.org/10.1016/B978-0-08-102528-4.00002-X>
- [55] Benedikt, F., Kuba, M., Schmid, J. C., Müller, S., & Hofbauer, H. (2019). Assessment of correlations between tar and product gas composition in dual fluidized bed steam gasification for online tar prediction. *Applied Energy*, 238, 1138–1149. <https://doi.org/10.1016/j.apenergy.2019.01.181>
- [56] Abdel-Galil, E. A., Rizk, H. E., & Mostafa, A. Z. (2016). Production and characterization of activated carbon from Leucaena plant wastes for removal of some toxic metal ions from waste solutions. *Desalination and Water Treatment*, 57(38), 17880–17891. <https://doi.org/10.1080/19443994.2015.1102768>
- [57] Caprariis, B. De, Filippis, P. De, Scarsella, M., Petrullo, A., & Palma, V. (2014). Biomass gasification and tar reforming in a two-stage reactor. *Energy Procedia*, 61, 1071–1074. <https://doi.org/10.1016/j.egypro.2014.11.1025>
- [58] Yu, H., Liu, Y., Liu, J., & Chen, D. (2019). High catalytic performance of an innovative Ni/magnesium slag catalyst for the syngas production and tar removal from biomass pyrolysis. *Fuel*, 254, 115622. <https://doi.org/10.1016/j.fuel.2019.115622>
- [59] Abdullah, B., Nisyah, A., Ilyas, S., & Tahir, D. (2019). Structural properties and bonding characteristics of honeycomb structure of composite ZnMnO₂ and activated carbon. *Journal of Applied Biomaterials and Functional Materials*, 17, 1-6. <https://doi.org/10.1177/2280800018820185>
- [60] Du, C., Liu, L., & Qiu, P. (2017). Importance of volatile AAEM species to char reactivity during volatile-char interactions. *RSC Advances*, 7(17), 10397–10406. <https://doi.org/10.1039/C6RA27485D>
- [61] Zhang, Y., Feng, D., Zhao, Y., Dong, H., Chang, G., Quan, C., Qin, Y. (2019). Evolution of char structure during in-situ biomass tar reforming: Importance of the coupling effect among the physical-chemical structure of char-based catalysts. *Catalysts*, 9(9), 711. <https://doi.org/10.3390/catal9090711>
- [62] Colomba, A. (2015). Production of Activated Carbons from Pyrolytic Biochar for Environmental Applications. PhD Thesis, University of Western Ontario.

- [63] Karaman, I., Yagmur, E., Banford, A., & Aktas, Z. (2014). The effect of process parameters on the carbon dioxide based production of activated carbon from lignite in a rotary reactor. *Fuel Processing Technology*, 118, 34–41.
<https://doi.org/10.1016/j.fuproc.2013.07.021>
- [65] Grebel, J. E., & (Mel) Suffet, I. H. (2007). Nitrogen-phosphorus detection and nitrogen chemiluminescence detection of volatile nitrosamines in water matrices: Optimization and performance comparison. *Journal of Chromatography A*, 1175(1), 141–144.
<https://doi.org/10.1016/j.chroma.2007.09.073>
- [67] Tipler, A. (2012). Sample Introduction Methods. *Gas Chromatography*, 187–219.
<https://doi.org/10.1016/B978-0-12-385540-4.00008-0>
- [68] Sigma Aldrich. Selecting a GC Column by a Specific Stationary Phase. Retrieved from: <https://www.sigmaaldrich.com/technical-documents/articles/analytical-applications/gc/select-proper-stationary-phase-gc.html>
- [69] Tidona, R. J., Nizam, A. A., & Cernansky, N. P. (1988). Reducing interference effects in the chemiluminescent measurement of nitric oxides from combustion systems. *Journal of the Air Pollution Control Association*, 38(6), 806–811.
<https://doi.org/10.1080/08940630.1988.10466421>
- [70] Rosemount Analytical (1999). Non-Dispersive Analyzer Module. Retrieved from: <https://www.emerson.com/documents/automation/manual-nga-2000-ndir-analyzer-module-sw-3-3-rev-a-rosemount-en-70104.pdf>
- [71] JoVE Science Education Database. Ultraviolet-Visible (UV-Vis) Spectroscopy. Retrieved from: <https://www.jove.com/v/10204/ultraviolet-visible-uv-vis-spectroscopy>
- [72] Hameed, B. S., Bhatt, C. S., Nagaraj, B., & Suresh, A. K. (2018). Chromatography as an efficient technique for the separation of diversified nanoparticles. *Nanomaterials in Chromatography: Current Trends in Chromatographic Research Technology and Techniques*, 503–518. <https://doi.org/10.1016/B978-0-12-812792-6.00019-4>
- [73] Wolfgang, W. J. (2016). Chemical analysis techniques for failure analysis: Part 1, common instrumental methods. *Handbook of Materials Failure Analysis with Case Studies from the Aerospace and Automotive Industries*, 279–307.
<https://doi.org/10.1016/B978-0-12-800950-5.00014-4>

- [74] Chemistry LibreTexts. UV-Visible Spectroscopy. Retrieved from:
[https://chem.libretexts.org/Bookshelves/Analytical_Chemistry/Book%3A_Physical_Methods_in_Chemistry_and_Nano_Science_\(Barron\)/04%3A_Chemical_Speciation/4.04%3A_UV-Visible_Spectroscopy](https://chem.libretexts.org/Bookshelves/Analytical_Chemistry/Book%3A_Physical_Methods_in_Chemistry_and_Nano_Science_(Barron)/04%3A_Chemical_Speciation/4.04%3A_UV-Visible_Spectroscopy)
- [75] Bardolf, R. (2017). Optimierung eines Produktgaswäschers bei der Biomassedampfvergasung im Zweibettwirbelschichtverfahren. PhD Thesis. Vienna University of Technology
- [76] Larsson, A.; Thunman, H.; Seemann, M.; Breitholtz, C.; Gunnarsson, I. (2018). Development of a methodology for measurements at the GoBiGas gasifier (Technical Report No. 466). Retrieved from:
<https://energiforskmedia.blob.core.windows.net/media/23897/development-of-a-methodology-for-measurements-at-the-gobigas-gasifier-energiforskrapport-2018-466.pdf>
- [77] Carpenter, D. L., Deutch, S. P., & French, R. J. (2007). Quantitative Measurement of Biomass Gasifier Tars Using a Molecular-Beam Mass Spectrometer: Comparison with Traditional Impinger Sampling. *Energy Fuels*, 21, 5, 3036–3043.
<https://doi.org/10.1021/ef070193c>
- [78] Hernandez-Eudave, M. T., Bonilla-Petriciolet, A., Moreno-Virgen, M. R., Rojas-Mayorga, C. K., & Tovar-Gómez, R. (2016). Design analysis of fixed-bed synergic adsorption of heavy metals and acid blue 25 on activated carbon. *Desalination and Water Treatment*, 57(21), 9824–9836. <https://doi.org/10.1080/19443994.2015.1031710>
- [79] Gluck, S. (1982). Performance of the Model 700A HallTM Electrolytic Conductivity Detector as a Sulfur-Selective Detector. *Journal of Chromatographic Science*, 103–108.
<https://doi.org/10.1093/chromsci/20.3.103>
- [80] Mitchell D. E. (1997). Analytical Chemistry of PCBs (Second Edition). CRC Press.
- [81] Ingenieria-Analitica. Agilent Model 255 Nitrogen Chemiluminescence Detector (NCD) Analysis of Adhesive Samples Using the NCD. Retrieved from:
http://www.ingenieria-analitica.com/downloads/dl/file/id/1136/product/211/agilent_model_255_nitrogen_chemiluminescence_detector_ncd_analysis_of_adhesive_samples_using_the_ncd.pdf
- [82] Kern, S., Pfeifer, C., & Hofbauer, H. (2013). Gasification of wood in a dual fluidized bed gasifier: Influence of fuel feeding on process performance. *Chemical Engineering Science*, 90, 284–298. <https://doi.org/10.1016/j.ces.2012.12.044>
- [85] Ali, M., Yan, C., Sun, Z., Gu, H., & Mehboob, K. (2013). Dust particle removal efficiency of a venturi scrubber. *Annals of Nuclear Energy*, 54, 178–183.
<https://doi.org/10.1016/j.anucene.2012.11.005>
- [86] A. Tadeu. (2018). Energy and sustainability (8th edition). WIT Press.
- [87] Speight, J. G. (2007). Natural gas – A basic handbook. Gulf Publishing Company. 161-192. <https://doi.org/10.1016/B978-1-933762-14-2.50012-1>

- [88] ThermoFisher. Materials Analysis Solutions for Research, Quality Assurance, Production and Teaching. Retrieved from: <https://assets.thermofisher.com/TFS-Assets/MSD/brochures/BR52986-materials-analysis-solutions-brochure.pdf>
- [89] Obaidullah, M. (2016). Formation, measurement and analysis of emissions from stack gas. Centre for Energy Studies.
- [90] Gazzani, M., & Manzolini, G. (2015). 11 - Using palladium membranes for carbon capture in integrated gasification combined cycle (IGCC) power plants. *Woodhead Publishing Series in Energy*, 221-246.
<https://doi.org/https://doi.org/10.1533/9781782422419.2.221>
- [91] Stewart, M. (2014). Gas Sweetening. Surface Production Operations. *Volume 2: Design of Gas-Handling Systems and Facilities*, 2, 433-539. <https://doi.org/10.1016/b978-0-12-382207-9.00009-3>
- [92] Wang, W., Padban, N., Ye, Z., Andersson, A., & Bjerle, I. (1999). Kinetics of ammonia decomposition in hot gas cleaning. *Industrial and Engineering Chemistry Research*, 38, 4175–4182. <https://doi.org/10.1021/ie990337d>
- [93] Abdoulmoumine N., Adhikari S., Kulkarni A. et al. (2015). A review on biomass gasification syngas cleanup. *Applied Energy*, 155, 294–307.
<https://doi.org/10.1016/j.apenergy.2015.05.095>
- [94] Asadullah M., (2014). Biomass gasification gas cleaning for downstream applications: A comparative critical review. *Renewable and Sustainable Energy Reviews*, 40, 118–132.
<https://doi.org/10.1016/j.rser.2014.07.132>
- [95] Woolcock P. J. & Brown R. C. (2013). A review of cleaning technologies for biomass-derived syngas. *Biomass and Bioenergy*, 52, 54–84.
<https://doi.org/10.1016/j.biombioe.2013.02.036>
- [96] Zhang W., Liu H., Ul Hai I. et al. (2012). Gas cleaning strategies for biomass gasification product gas. *International Journal of Low-Carbon Technologies*, 7, 2, 69–74. <https://doi.org/10.1093/ijlct/ctr046>

